

Taxonomic revision, morphology, and genetic variability of *Holothuriophilus trapeziformis* Nauck, 1880 (Decapoda: Pinnotheridae) from the Pacific coast of Mexico

Fernando Cortés-Carrasco¹, Manuel Elías-Gutiérrez^{Corresp., 2}, María del Socorro García-Madrigal³

¹ Aquatic Ecology and Systematics, El Colegio de la Frontera Sur, Chetumal Unit, Chetumal, Quintana Roo, Mexico

² Aquatic Ecology and Systematics, El Colegio de la Frontera Sur, Chetumal, Quintana Roo, Mexico

³ Campus Puerto Ángel, Universidad del Mar, Puerto Ángel, Oaxaca, Mexico

Corresponding Author: Manuel Elías-Gutiérrez

Email address: melias@ecosur.mx

Background. *Holothuriophilus trapeziformis* Nauck, 1880 is a holothurian-dweller Pinnotherid crab and represents one of the two species of the genus, which is distributed along the Pacific coast of America. Currently, only one morphological character separates both species because, since 1880, only the females were known. Furthermore, the original description of *H. trapeziformis* and its subsequent descriptions are incomplete or ambiguous and genetic information for this species does not exist. Our goal here is to describe for the first time the *H. trapeziformis* male morphology, discuss the morphological variations observed and clarify the taxonomic status of the species, and provide a genetic comparison based on the DNA barcoding.

Methods. We used the integrative taxonomy to re-describe *H. trapeziformis*, including a complete morphological description of the male and female. We also compared, the intraspecific morphological variability and conducted a genetic analysis based on comparing of the COI gene among different sequences of the related Pinnotheridae prepared by us and available public databases.

Results. *Holothuriophilus trapeziformis*, as any decapod, has a strong sexual dimorphism. Fifty-five specimens collected on the Pacific coast of Mexico were examined, and the DNA barcodes were compared. *H. trapeziformis* is confirmed as a different species from *H. pacificus* by the general shape of the carapace, the previously known interdactilar gape condition, the ornamentation of the pincers fingers, and by the shape of the male abdomen and its first gonopod, also the interspecific COI divergences are >3%. Morphological variations coincide with COI, and a haplotype network resolution defined one clade and two subgroups. Genetic analyses determined a structure population with 22 haplotypes among regions with a gene flow of the possible ancestral haplotype from south to north. An emerging allopatric differentiation process is showed by both the species morphology and barcoding. Results coincided with the Barcode Index Number (BIN) assigned to this species (BOLD: ADE9974). Moreover, *H. trapeziformis* is recorded for the first time within the intestine of its host, the sea cucumber *Holothuria (Halodeima) inornata* Semper, and its distribution range on the Mexican Pacific coast was extended.

1
2
3
4
5
6
7
8
9
10
11
12
13
14
15
16
17
18
19
20
21
22
23
24
25
26
27
28
29
30
31
32
33
34

Taxonomic revision, morphology, and genetic variability of *Holothuriophilus trapeziformis* Nauck, 1880 (Decapoda: Pinnotheridae) from the Pacific coast of Mexico.

Fernando Cortés-Carrasco¹, Manuel Elías-Gutiérrez^{1*}, María del Socorro García-Madriral²

¹Departamento de Sistemática y Ecología Acuática, Zooplancton y Oceanografía. El Colegio de la Frontera Sur unidad Chetumal, Avenida Centenario km 5.5, Apdo. Postal 424, 77000, Chetumal, Quintana Roo, México.

²Laboratorio de Sistemática de Invertebrados Marinos (LABSIM), Universidad del Mar, Campus Puerto Ángel, Ciudad Universitaria, Apdo. Postal 47, 70902, Puerto Ángel, Oaxaca, México.

*Corresponding author:
Manuel Elías-Gutiérrez
melias@ecosur.mx

35 **Abstract**

36 **Background.** *Holothuriophilus trapeziformis* Nauck, 1880 is a holothurian-dweller Pinnotherid
37 crab and represents one of the two species of the genus, which is distributed along the Pacific coast
38 of America. Currently, only one morphological character separates both species because, since
39 1880, only the females were known. Furthermore, the original description of *H. trapeziformis* and
40 its subsequent descriptions are incomplete or ambiguous and genetic information for this species
41 does not exist. Our goal here is to describe for the first time the *H. trapeziformis* male morphology,
42 discuss the morphological variations observed and clarify the taxonomic status of the species, and
43 provide a genetic comparison based on the DNA barcoding.

44 **Methods.** We used the integrative taxonomy to re-describe *Holothuriophilus trapeziformis*,
45 including a complete morphological description of the male and female. We also compared, the
46 intraspecific morphological variability and conducted a genetic analysis based on comparing of
47 the COI gene among different sequences of the related Pinnotheridae prepared by us and available
48 public databases.

49 **Results.** *Holothuriophilus trapeziformis*, as any decapod, has a strong sexual dimorphism. Fifty-
50 five specimens collected on the Pacific coast of Mexico were examined, and the DNA barcodes
51 were compared. *H. trapeziformis* is confirmed as a different species from *H. pacificus* by the
52 general shape of the carapace, the previously known interdactilar gape condition, the
53 ornamentation of the pincers fingers, and by the shape of the male abdomen and its first gonopod,
54 also the interspecific COI divergences are >3%. Morphological variations coincide with COI, and
55 a haplotype network resolution defined one clade and two subgroups. Genetic analyses determined
56 a structure population with 22 haplotypes among regions with a gene flow of the possible ancestral
57 haplotype from south to north. An emerging allopatric differentiation process is showed by both

58 the species morphology and barcoding. Results coincided with the Barcode Index Number (BIN)
59 assigned to this species (BOLD: ADE9974). Moreover, *H. trapeziformis* is recorded for the first
60 time within the intestine of its host, the sea cucumber *Holothuria (Halodeima) inornata* Semper,
61 and its distribution range on the Mexican Pacific coast was extended.

62 **Introduction.**

63 Pinnotherids (Crustacea: Pinnotheridae) are true decapod crabs, which show a conspicuous sexual
64 dimorphism, notably different morphological states of development and complex ecological
65 relationships with different invertebrates, and can also be found in free life (Schmitt et al. 1973;
66 Ocampo et al. 2011; Becker & Türkay 2017). Thirteen species are known to be endobiotic with
67 sea cucumbers (Ng & Manning 2003). Of them, *Holothuriophilus trapeziformis* Nauck, 1880, is
68 one of the two species of pinnotherids crabs described for the genus (Manning 1993); however,
69 his taxonomic status remains incomplete because male morphology is unknown and the available
70 information about the female illustrations shows some inconsistencies. These situations have
71 caused the differentiation of both species to be based on a single morphological character (Campos,
72 Peláez-Zárate & Solís-Marín 2012) that could be subjective. It should be added that, to date, there
73 is no genetic information related to *H. trapeziformis*.

74 *Holothuriophilus* Nauck, 1880 from the Pacific coast of America, was established with *H.*
75 *trapeziformis* from Mazatlan, Mexico, and includes *H. pacificus* (Poeppig, 1836) from
76 Talcahuano, Chile (Manning 1993). Both species are associated with sea cucumbers (Garth
77 1957; Campos, Peláez-Zárate & Solís-Marín 2012). Also, *Pinnaxodes mutuensis* Sakai, 1939,
78 from Aomori Bay, Japan (Takeda & Masahito 2000) and *P. tomentosus* Ortmann, 1894, from
79 Brazil have been considered as belonging to *Holothuriophilus* (Melo & Bohes 2004; Ng, Guinot
80 & Davie 2008). However, their definitive status is currently under revision due to differences in

81 diagnostic characters and for being associated with mollusks as a host (Campos, Peláez-Zárate &
82 Solís-Marín 2012).

83 *Holothuriophilus* is diagnosed by its transversally elongated carapace, wider anterior to middle
84 portion; its short, robust and compressed walking legs, with the dorsal margin cristate; and the
85 third maxilliped, with the ischiomerus indistinguishably fused (Garth 1957; Manning 1993; Ng &
86 Manning 2003; Campos, Peláez-Zárate & Solís-Marín 2012).

87 So far, *Holothuriophilus trapeziformis* can only be differentiated from *H. pacificus* based on a
88 single morphological character and by an ecological condition related to the host specificity. The
89 former species has a narrowed opening when the pincers' fingers are closed and its ecological
90 host is the sea cucumber *Holothuria (Halodeima) inornata* Semper, but in the latter species the
91 finger's gap is conspicuous and its host corresponds to *Athyonidium chilensis* (Semper) (=
92 *Eucyclus chilensis*), another sea cucumber (Garth 1957; Campos, Peláez-Zárate & Solís-Marín
93 2012; Honey-Escandón & Solís-Marín 2018).

94 Also, Nauck (1880) did not designate a holotype when he described *H. trapeziformis*, the
95 original description did not provide enough information, and the host identity was erroneously
96 determined. Moreover, the female syntypes were deteriorated over time and the male was
97 unknown (Bürger 1895; De Man 1887; Ng & Manning 2003). Later, Manning (1993), Ng &
98 Manning (2003) and Ahyong & Ng (2007) examined the syntype series to complete the
99 diagnosis and designated a lectotype which was described and illustrated. However, there are
100 inconsistencies between their illustrations and the diagnostic characters are not informative when
101 considering the information available for *Holothuriophilus pacificus*. In addition, for 84 years *H.*
102 *trapeziformis* had not been collected again until Caso (1958, 1964, 1965). She collected four
103 pinnotherids determined as *Pinnixa barnharti* (not *Pinnixa barnharti* Rathbun, 1918) associated

104 with *Holothuria inornata* Semper and *H. kefersteinii* (Selenka) (= *H. riojai* Caso, 1964). Thirty-
105 four years later, one of Caso's specimens was determined as *Holothuriophilus* sp. by Campos,
106 Díaz & Gamboa-Contreras (1998). More recently Campos, Peláez-Zárate & Solís-Marín (2012)
107 updated the species diagnosis and made a review of the genus. Finally, Honey-Escandón &
108 Solís-Marín (2018) confirmed the ecological association between *H. trapeziformis* and
109 *Holothuria inornata*, but Caso's (1958, 1965) records of *Holothuria kefersteinii* as a host
110 remains uncertain because the field collection data does not correspond with the material
111 reviewed by Honey-Escandón & Solís-Marín (2018), and the location of these pinnotherids and
112 their holothurian hosts is unknown (F Solís-Marín, 2018, pers. comm.).
113 For *Holothuriophilus trapeziformis* there is currently no data on genetic information and on its
114 historical demography, contrary to *H. pacificus* that has information related to the COI gene
115 sequence for one specimen from the shoreline in southern Chile (CFAD062-11;
116 boldsystems.org). In this context, sequencing of approximately 650 bp region of the
117 mitochondrial Cytochrome Oxidase 1 gene (COI) has been promoted to conform a standardized
118 DNA barcode system with the aim of being one more tool for the identification of biological
119 species with many applications in diverse fields of knowledge (Hebert et al. 2003; Hajibabaei et
120 al. 2007). In spite of the difficulty to work with COI regarding the debate about the acceptance of
121 one molecular marker as an accurate character to delimit a species (Will & Rubinoff 2004), it has
122 been considered the best marker for identification in other decapods (Spielmann et al. 2019) and
123 the utility of the DNA Barcoding (COI sequence) has been useful to delimit other pinnotherids
124 (Ocampo et al. 2013; Perez-Miguel et al. 2019), brachyuran larvae (Brandão et al. 2016), and
125 other crustacean taxa (Costa et al. 2007; Matzen da Silva et al. 2011).

126 Considering that integrative taxonomy based on morphological and molecular data, is
127 increasingly useful to define and delimit biological species with greater certainty, the goal of this
128 study is, therefore, to define the taxonomic status of *Holothuriophilus trapeziformis* by
129 completing the information on the species with the description of the male, revising of the
130 morphological variability in both sexes, updating the range of distribution, and establishing a
131 baseline of genetic variability and historical demography based on the mitochondrial COI gene.
132 Finally, this information will provide new diagnostic characters that will allow a clearer
133 separation of both species of *Holothuriophilus* from the Pacific coast of America.

134 **Material & methods**

135 **Morphology**

136 Fifty-two crabs belonging to the *H. trapeziformis* were extracted from the coelom and intestine
137 of the sea cucumber *Holothuria inornata*. Hosts were manually collected through skin and
138 SCUBA diving at a maximum depth of 10 meters in Sinaloa, Guerrero, and Oaxaca, Mexico.
139 The collected material was labeled and fixed according to the Elías-Gutiérrez et al. (2018)
140 protocol for the tissue preservation. Furthermore, due to the size of the specimens and the
141 thickness of the cuticle, the preservative was injected into the body of the crabs and the hosts
142 with individual insulin syringes to preserve DNA quality for subsequent molecular studies
143 described later in the molecular data section.

144 All biological material (Table S1) was classified and deposited in the Scientific Collection of
145 Marine Invertebrates of the Laboratorio de Sistemática de Invertebrados Marinos (LABSIM)
146 from Universidad del Mar (UMAR), Oaxaca, Mexico (OAX-CC-249-11). Hosts were identified
147 with specialized literature (Solís-Marín et al. 2009; Honey-Escandón & Solís-Marín 2018).

148 For the analysis of the taxonomic status of *Holothuriophilus trapeziformis* specialized literature
149 from Nauck (1880), Manning (1993), Ng & Manning (2003), Ahyong & Ng (2007), and
150 Campos, Peláez-Zárate & Solís-Marine (2012) was reviewed. Likewise, for *H. pacificus*,
151 Poeppig (1836), Nobili (1901), Rathbun (1918) and Garth (1957), were reviewed.

152 Field permit for collections with non-commercial scientific research purposes was issued by
153 Secretaría de Agricultura, Ganadería, Desarrollo Rural, Pesca y Alimentación (SAGARPA) and
154 Comisión Nacional de Acuacultura y Pesca (CONAPESCA) (Collecting permit: PPF/DGOPA-
155 301/17).

156 The species description follows the terminology of Campos et al. (2012) and Davie, Guinot &
157 Ng (2015), this last one mostly for the general shape of the carapace, and setae terminology of
158 Garm & Watling (2013). Drawings were made with the help of a lucid camera and then
159 digitalized in a vector format. Pictures were taken with a digital camera Nikon D5100. Measures
160 are given in millimeters and the latitude and longitude were obtained from Google Earth™.

161 Because we were only able to obtain nine specimens (three males and six females) from the type
162 locality, in contrast to 47 (six males and 41 females) from the southern region, and due to
163 morphological variability observed among individuals of the same sex and between them, as well
164 as within and among geographic regions, it was necessary to standardize the observations of the
165 variation with specimens at the same stage of development. The shared stage of development
166 between the three regions (Sinaloa, Guerrero, and Oaxaca) corresponded to males and ovigerous
167 females with a carapace width measurement equal to eight millimeters. To standardize the
168 observations, the specimen and the dissected pieces were mounted on a plastic clay base to make
169 the drawings. Punctually, for the carapace contour, these were mounted in such a way that the
170 dorsal view of the posterior margin line of the carapace still can be observed. For the Mxp3, an

171 attempt was made to extract it from its base to obtain both endopod and exopod, and to mount it
172 with the articles in the same perspective. The cutting edge of the fingers chelae were cleaned of
173 dirt in order to view all the teeth. The first gonopod was extracted from its base and the setae
174 cleaned of dirt.

175 Abbreviations used in the text: CL, carapace length (taken as the middle line from the frontal
176 margin to the posterior margin of the carapace); CW, carapace width (measured in its medium-
177 anterior portion); Mxp2, second maxilliped; Mxp3, third maxilliped; P2–5, walking legs 1 to 4.

178 Acronyms used in the text: BOLD, barcode of life database (boldsystems.org); BIN, barcode
179 index number (*sensu* Ratnasingham & Hebert, 2013); BOLD-ID, Specimen ID in the Barcode of
180 Life Data System; CNE-ICML-UNAM, National Collection of Echinoderms of the Institute of
181 Marine Sciences and Limnology of the National Autonomous University of Mexico; DC-NHM,
182 Division of Crustacea, Natural History Museum, Smithsonian Institution; SMF-ZMG,
183 Senckenberg Museum für Naturkunde, Zoologisches Museum Göttingen University, Humboldt
184 Universität, Berlin; UABC, Autonomous University of Baja California, Mexico; UMAR,
185 Universidad del Mar campus Puerto Angel, Oaxaca, Mexico.

186 Collectors: AEV, Aidé Egremy Valdés; AGF, Andrea Glockner Fagetti; CCA, Carlos Cruz
187 Antonio; AHM, Adanely Hernández Muñoz; FBV, Francisco Benítez Villalobos; FCC, Fernando
188 Cortés Carrasco; HMC, Humberto Mesa Castillo; KFL, Karen Lizbeth Flores López; KMB,
189 Karen Mesa Buendía; RGF, Rebeca Granja Fernández; VCH, Valeria Chavez García.

190 **DNA extraction and PCR amplification**

191 From the biological material collected in the field and some other taken from the OAX-CC-249-
192 11 collection, genomic DNA was extracted from different tissue samples. For the crabs, muscle
193 of the walking legs, chelae, or eggs were used. For the sea cucumber hosts, underlying muscle

194 from the dorsolateral body wall and/or internal longitudinal ventral muscle were used. Tissues
195 were placed into 96-well microplates with a drop of 96% ethanol, and DNA extraction was
196 carried out following the standard glass fiber method of a mix of Proteinase K with invertebrate
197 lysis buffer according to Ivanova, De Waard & Hebert (2006). Following DNA extraction, the
198 PCR mixture with a final volume of 12.5 μ l, contain 2 μ l of Hyclone ultrapure water (Thermo
199 Fisher Scientific), 6.25 μ l of 10% trehalose (previously prepared: 5 g D-(+)- trehalose dihydrate
200 (Fluka Analytical) in 50 ml of total volume of molecular grade ddH₂O), 1.25 μ l of 10X PCR
201 Platinum Taq buffer (Invitrogen), 0.625 μ l of 50 μ mol/L MgCl₂ (Invitrogen), 0.0625 μ l of 10
202 μ mol/L dNTP (KAPA Biosystems), 0.125 μ l of each 10 μ mol/L primer, 0.06 μ l of PlatinumTaq
203 DNA polymerase (Invitrogen) and 2 μ l of DNA template. All specimens were amplified with the
204 Zooplankton primers (ZplankF1_t1 and ZplankR1_t1, see Prosser *et al.*, 2013 for details). The
205 reactions were cycled at 94°C for 1 min, followed by five cycles of 94°C for 40 seconds, 45°C
206 for 40 seconds and 72°C for 1 min, followed by 35 cycles of 94°C for 40 seconds, 51°C for 40
207 seconds and 72°C for 1 min, with a final extension of 72°C for 5 min. PCR products were
208 visualized on a pre-cast 2% agarose gels (E-Gel[®] 96 Invitrogen), and the most intense positive
209 products were selected for sequencing.

210 **Sequencing and DNA barcode**

211 Selected PCR products were sequenced using a modified (Hajibabaei et al. 2005) BigDye[®]
212 Terminator v.3.1 Cycle Sequencing Kit (Applied Biosystem, Inc.), and then sequenced
213 bidirectionally on an ABI 3730XL automated capillary sequencer using M13F and M13R
214 sequence primers at the Biology Institute at the National Autonomous University of Mexico and
215 at the Eurofins Genomics Louisville Laboratory. Sequences were edited using CodonCode[®] v
216 3.0.1 (CodonCode Corporation, Dedham, MA, USA) and uploaded to BOLD. In some cases, the

217 original forward and reverse tracers uploaded to BOLD were checked again, consensus assembly
218 was generated, and edited manually with Sequencher[®] 4.1.4. (Gene Codes Corporation, Ann
219 Arbor, MI, USA), and then they were aligned using BioEdit[®] (Hall 1999).

220 **Phylogeny and distance analysis**

221 COI sequences generated for *Holothuriophilus trapeziformis* in this study were compared with
222 COI sequences from other pinnotherids collected in the Eastern Pacific coast of America,
223 considered as an outgroup and available in BOLD and/or GeneBank (Table S2). Sequence data,
224 trace files, and primer details for all *H. trapeziformis* specimens and for the outgroup species are
225 available under the dataset name PINMX1HT (“Htrapeziformis from Mexico”; DOI:
226 [dx.doi.org/10.5883/DS-PINMX1HT](https://doi.org/10.5883/DS-PINMX1HT)) in the Barcode of Life Data System (barcodinglife.org).
227 Additionally, *Holothuriophilus trapeziformis* sequences were uploaded to GenBank
228 (<https://www.ncbi.nlm.nih.gov/>).

229 To infer the phylogenetic relationships, the best-fitting evolution model of nucleotide
230 substitution for distance based on COI alignments was established on the Maximum Likelihood
231 (ML) for 24 different nucleotide substitution models, selected according to the Akaike (AIC) and
232 Bayesian (BIC) criterion (Darriba et al. 2011), and tested using jModelTest[®] 2.1.10 (Posada &
233 Buckley 2004). The final phylogenetic topology was obtained with nodal support for the
234 resulting branches estimated with 1000 bootstrap replicates in MEGA[®] 6.0 (Tamura et al. 2013).
235 Finally, the resulting topology was edited, and a simplified tree was constructed using FigTree[®]
236 (Rambaut 2016). Also, interspecific COI genetic distances for the dataset were estimated using
237 the Kimura-2 parameters distance method in MEGA[®] 6.0 (Tamura et al. 2013). Values greater
238 than 3% were considered as threshold for the delimitation of species (Hebert et al. 2003).

239 **Intraspecific DNA polymorphisms and historical demography**

240 In order to determine the genetic variation within the *Holothuriophilus trapeziformis* group, 37
241 sequences from the Pacific coast of Mexico were aligned with MUSCLE routine, and
242 intraspecific genetic divergences were obtained using the Kimura 2-parameter substitution model
243 with a bootstrap method in MEGA[®] 6.0 (Tamura et al. 2013).
244 Genetic diversity was estimated with the haplotype diversity (Hd), number of haplotypes (H),
245 nucleotide diversity (π), number of polymorphic or segregating sites (S), average number of
246 nucleotide differences between pairs of sequences (k), guanine and cytosine content (G+C), and
247 all the haplotypes of the genetic variants of COI within species were obtained using DnaSP[®]
248 v6.12.01 (Rozas et al. 2003, 2017) (<http://www.ub.edu/dnasp/>).
249 The genetic differentiation between localities (Sinaloa, Guerrero, Oaxaca) was analyzed with the
250 aid of a fixation index Phist (Φ_{ST} test; with a 10000 permutations for pairwise genetic distance)
251 using Arlequin[®] v3.5.2.2 (Excoffier & Lischer 2015)
252 (<http://cmpg.unibe.ch/software/arlequin35/>). Phist values ranged from 0 to 1, and can be
253 interpreted according to a scale range of 0.05 as low, 0.05 to 0.15 as moderate, 0.15 to 0.25 as
254 great, and above 0.25 as very great; though there is no strict consensus about that scale range
255 (Hartl & Clark 1997). This metric considers the haplotype phylogenetic distance and is more
256 robust when the genetic diversity within the localities increases (Munguia-Vega et al. 2014).
257 Additionally, the spatial relationships between the sampled localities were analyzed through the
258 Spatial Analysis of the Molecular Variance (SAMOVA) evaluating the most likely number of
259 groups ranging from k=1 to K=2, and significance of Φ statistics was tested by 100000
260 permutations using SAMOVA 2.0 software (Dupanloup et al. 2002). The correlation between
261 genetic divergence and geographical distance among localities (isolation by distance) was tested

262 with a Mantel test performed in XLSTAT v. 2020.1 (<https://www.xlstat.com/en/>), the p-value
263 was estimated by 10000 Monte Carlo simulations.

264 Graphical explanation for biogeographical relationships of COI sequences was represented with
265 a PopART haplotype network (<http://popart.otago.ac.nz/index.shtml>) considering the parsimony
266 criterion (Clement et al. 2002; Leigh & Bryant 2015).

267 Mismatch distribution obtained with DnaSP[©] was used to deduce if a population has undergone
268 sudden population expansion; a unimodal distribution indicates recent population expansion with
269 little lineage loss, whereas no defined multimodal distribution indicates a constant size growth
270 with stochastic lineage loss (Harpending et al. 1993). A goodness of fit between the mismatch
271 distributions was tested under a coalescent model with the Raggedness index (r) and R_2 function
272 in Arlequin[©], because these are considered powerful metrics to determine population change
273 when sample size is small (Harpending 1994; Ramos-Onsins & Rozas 2002). In order to
274 examine the signature of population demographic changes in *Holothuriophilus trapeziformis*
275 sample, we used the Tajima's D statistic with a 1000 coalescent permutations to infer if the data
276 conformed to expectations of neutrality model or if it departed from them; where a statistic near
277 to zero indicates a constant-size population, significant negative values indicate a sudden
278 expansion, and significant positive values indicate recent population bottleneck or a population
279 subdivision (Ramos-Onsins & Rozas 2002).

280 **Results**

281 Here we analyzed the morphology of 56 specimens coming from three coastal regions in the
282 Mexican Pacific in which the type locality is included; of them, only 51 were processed for the
283 molecular analysis. All the material is listed in Table S1. Detailed morphological revision
284 allowed us to determine notable variations, mostly on the carapace general shape, features of the

285 first male gonopod, and in the pincers chelae ornamentation. Northern type locality morphology
286 shows a notable variation in the general carapace outline shape and general appearance which
287 looks more stout and eroded with respect to that of the southern specimens; however, all
288 specimens show features that define *Holothuriophilus trapeziformis* according to Ng & Manning
289 (2003), Campos, Peláez-Zárate & Solís-Marín (2012). Besides that, previously undescribed
290 structures like the Mxp2 and male second gonopod plus the genetic data resolution, confirm that
291 all the revised material corresponds with the *H. trapeziformis*. Complete morphology description
292 of the male and discussion of character variations in both sexes are annotated in the Systematic
293 section and genetic analyses are annotated after that.

294 **Systematics**

295 Infraorder Brachyura Latreille, 1802

296 Family Pinnotheridae De Haan, 1833

297 Genus *Holothuriophilus* Nauck, 1880

298 *Holothuriophilus*. — Manning, 1993: 225 (First genus diagnosis).

299 **Diagnosis (modified from Manning 1993)**. Carapace broader than long, **widest on mid**
300 **anterior portion, transversely** subrectangular, **subovate or subtrapezoidal**. Third maxilliped
301 with ischium and merus indistinguishable fused; exopod with **one segmented** flagellum;
302 **endopod** palp 3-segmented; propodus shorter than carpus, conical; subspatulate dactylus
303 articulates basally on propodus, extending beyond end of propodus. Dactyli of walking legs
304 similar and subequal, short. Abdomen of seven segments in both sexes.

305 *Holothuriophilus trapeziformis* Nauck, 1880

306 (Figs. 1A–G, 2A–D, 3A–F 4A–F, 5A–D)

307 *Holothuriophilus trapeziformis* Nauck, 1880: 24, 66 (Brief diagnosis of cephalothorax and
308 Mxp3, type locality Mazatlan, Mexico, indicates association with *Holothuria maxima* Semper).—
309 —De Man 1887: 721–722 (Female syntype redescription, CW = 13.8 mm, CL = 10.5 mm).—
310 Manning 1993: 524–528, Fig. 3C (Reinstates and diagnoses of the genus).—Ng & Manning
311 2003: 903, 916–918, Fig. 7C–F, (Designates female lectotype: SMF-ZMG 67/565a, CW = 7.7
312 mm, LC = 4.8 mm, illustration of Mxp3 and walking legs).—Ahyong & Ng 2007: 213–214, Fig.
313 20, (Illustrate the general shape of the body, cheliped and Mxp3 of the lectotype SMF-ZMG 170
314 (Go565a), CW = 7.7 mm, CL = 4.8 mm).—Campos, Peláez-Zárate & Solís-Marín 2012: 57–62,
315 Figs. 1A, B, 2A–D (Record specimens from Punta Tiburon, Mazatlan, Sinaloa, Mexico,
316 associated with *Holothuria lubrica* and *H. inornata* and from Ixtapa, Guerrero, Mexico,
317 associated with *Holothuria kefersteinii* and *H. inornata* deposited in the CNE-ICMyL-UNAM
318 Collection).

319 *Pinnotheres trapeziformis* Bürger 1895: 380–381, plate 9, Fig. 26, plate 10, Fig. 25 (Brief
320 description of one female (CW = 14 mm, CL = 10 mm) associated with *Holothuria maxima*
321 Semper from unknown locality, and one specimen erroneously determined as a male (CW = 5
322 mm, CL = 8.5 mm) associated with *Holothuria inornata* Semper, from Mazatlan, Mexico).—
323 Adensamer 1887: 107 (Provides the catalog number for the SMF).—Tesch 1918: 285 (list of
324 species).—Schmitt, McCain & Davidson 1973: 5, 13, 89 (Annotated checklist of the
325 Pinnotheridae from the DC-NHM).

326 *Pinnotheres trapeziformis* Balss 1957: 1417 (not 1956 *vide* Schmitt, McCain & Davidson 1973).

327 *Pinnixa barnharti* (no Rathbun, 1918) Caso 1958: 329 (First record since Nauck (1880) of a
328 specimen from playa El Almacén, Guerrero, identified by Rioja), 1965: 254–26 (Second record
329 of three specimens from playa Las Gatas, Guerrero, identified by Rioja).

330 *Holothuriophilus* sp. Campos, Díaz & Gambóia-Contrera 1998: 377, Fig. 1E (Corrects as
331 *Holothuria* sp. the name of a *Pinnixa barnharti* specimen recorded by Caso (1965) from
332 Guerrero, illustration of the Mxp3).

333 **Material examined:** 56 specimens: 25 ovigerous females, 22 females, nine males (Table S1).

334 **General distribution:** Tropical Eastern Pacific (Mexico).

335 **Previous records:** Mazatlan, Punta Tiburon (Sinaloa); Ixtapa (Guerrero).

336 **New records:** playa Pinitos (Sinaloa); playa Nudista, playa Zacatoso, playa Caleta de Chon
337 (Guerrero); playa Agua Blanca, playa Coral, playa Camaron, playa Panteón, playa Estacahuite,
338 playa La Tijera, bahia San Agustin, playa El Tejon (Oaxaca).

339 **BIN:** BOLD:ADE9974

340 **Size range (mm):** Males: CW = 5.5–11, CL = 3.2–7; females: CW = 5.1–11, CL = 3–7;
341 ovigerous females: CW = 7.3–13, CL = 5–8.

342 **Diagnosis (modified from Campos, Peláez-Zárte & Solís-Marín 2012).** Carapace
343 transversally elongated, widest anterior to middle portion, broader than long, **general shape**
344 **transversely suboval or subtrapezoidal**; anterolateral margin cristate, **with a hepatic notch**
345 **which has a vanished blunt tooth, notch sometimes visible only in lateral view**; front under
346 postfrontal ridge, deflexed, emarginated, its margin scarcely visible in dorsal view. Third
347 maxilliped with ischium merus indistinguishably fused, palp 3-segmented; carpus subequal in
348 length to subtrapezoidal propodus; spoon-shaped **or suboblong** dactylus articulated on medial
349 ventral third of propodus; tip of dactylus slightly overreaching tip of propodus; exopod with one-
350 segment flagellum. Cheliped merus, carpus **inner surface** densely setose; **propodus ventral**
351 **inner margin with a row of short seta**; propodus and dactylus almost meeting when closed;
352 **dactylus cutting edge with proximal denticles, a conspicuous tooth and a distal convex or**

353 **acute projection.** Walking legs robust, similar in shape, segments compressed, **dorsal surface**
354 **cristate; merus dorsal surface of W1, 3 and 4 with setae, W2 without seta;** carpi and propodi
355 subequal; dactyli shorter than preceding articles, similar and subequal, last pair shorter than
356 preceding. Abdomen with 6 somites plus free telson; **on male, margin of somite 4 to 6 concave,**
357 **telson subrounded. Male first gonopod notably curved outward from its mid-distal portion.**
358 **Description:** Male (Fig 1A, B, C; UMAR-DECA-308; CW = 11 mm, CL = 7 mm): Carapace,
359 transversely subtrapezoidal, wider than long, CW/CL ratio ca. 1.4 to 1.6, mid-anterior portion
360 wider; anterolateral margins slightly projected, cristated, a hepatic notch with a blunt middle
361 tooth (Figs. 2A, B; bold arrow); dorsal surface convex, smooth, without defined regions; mid-
362 posterior and posterolateral surface with microscopic pits of variable size and pilosity (Figs. 2A,
363 C; hollow circles and dots); inferior lateral margin with abundant plumose setae (Fig. 2A; simple
364 lines represent the enlarged schematic setae). Front bilobed, scarcely visible in dorsal view,
365 margin granulated, surface slightly pubescent (Fig. 2B; dots). Orbits small, completely filled by
366 eyes; eyes pigmented; ocular peduncle scarcely pubescent. Antennules robust; peduncle 2-
367 segmented, biflagellate, transversely folded into the fossae; superior flagellum 2-articles, second
368 article the longest, tapering distally, with six apical setae (Fig. 3Ba); inferior flagellum conic,
369 with four articles decreasing in size, article one to three with a transverse line of simple setae,
370 fourth article with two transverse lines of simple seta (Fig. 3Bb). Antennae long, slender, with 12
371 articles denuded of setae, last article with short apical setae (Fig. 3A). Pterygostomian region
372 pubescence (Fig. 2B; fine dots). Buccal frame trapezoidal, completely covered by the Mxp3.
373 Mxp2 endopod 5-articles, with setae (Fig. 3Ca), dactylus subrounded and shorter than propodus
374 (Fig. 3C; black arrowhead); exopod 1-article, wider distally, external surface with an elevated
375 ridge (Fig. 3Cb), flagellum with long apical setae (Fig. 3Cc), epipodite long, distal margin

376 rounded (Fig. 3Cd). Mxp3 ischiomerus fused without suture line, width-length ratio= 0.7,
377 external margin convex with setae, internal margin with a medial conspicuous projection (Fig.
378 3Da; white arrow); carpus subconial, external margin with short setae; propodus subconical (Fig.
379 3Dc); dactylus subspatuliform, wider distally (Fig. 3D; black arrowhead), slightly overreaching
380 propodus, external surface with short plumose setae, external margin with long plumose setae;
381 exopod 1-article, external margin and external surface with short simple setae, flagellum slender,
382 with plumose long setae (Fig. 3E). Sternal third plate with anterior margin sinuous, anterolateral
383 angles with crenu-denticulated margin (Fig. 2C; black arrow), surface scarcely pilose (Fig. 2C;
384 dots); fourth plate slightly globose, surface with microscopic pits (Fig. 2C; hollow circles), distal
385 external angle curved outward, margin crenu-denticulated (Fig. 2C; white arrow). Chelipeds
386 subequals (Figs. 1A–C); merus external surface and carpus anterior margin with plumose setae;
387 chelae width and length subequal, ventral margin microscopically granulated (Fig. 3F, 6C;
388 dashed arrow), dorsal margin slightly cristate and bent inwards; fingers wider than long, length
389 equal, spoon-tipped, tip acute (Fig. 3F), interdactylar gap narrow (vg. Fig. 6C); movable finger
390 shorter than fixed finger, crossed inward when the pincer is closed (vg. Fig. 6C), cutting edge
391 sinuous, with three medial teeth (Fig. 3F; bold arrow) and a mid-distal convex projection (Fig.
392 3F; white dashed arrow); fixed finger cutting edge with nine teeth, faint lamella over the smooth
393 portion of the cutting edge (Fig. 3F; dotted arrow), ventral inner surface with short setae. Walking
394 legs similar, relative length $W3 > W2 > W1 > W4$, segments short, robust, compressed, dorsal
395 margin cristate, ventral surface with plumose setae; merus dorsal margin on W1, W3, W4 with
396 plumose setae, on W2 without setae; dactylus curved, stout, tips acute; W1–W3, dactylus
397 subequal than propodus, of W4 shorter than its propodus (Figs. 1B, 2A). Abdomen symmetrical,
398 subtriangular, six free somites plus a telson, margin with short setae, lateral margin from

399 segments 4–6 slightly concave and narrowing, telson subrounded (Figs. 4B). First gonopod
400 slender, margins sinuous, mid-distal portion notably curved outwards, surface with abundant
401 plumose setae (Fig. 4D). Second gonopod small, flagellum curved outwards, slightly bent
402 inwards, tip pointing upwards, margins convex with a shallow notch (Fig. 2F; black arrow).

403 **Color in life:** Body beige or creamy white, dorsal surface of carapace and chelipeds carpus, and
404 on the external surface of the chelae with red patches. In fixed and preserved specimens this
405 pattern of color remains or it could change from red to light or dark brown.

406 **Habitat:** Marine. Associated with the sea cucumber *Holothuria (Halodeima) inornata*, living in
407 its coelom and inside its intestine. This holothurian inhabits rocky-sand bottoms in shallow
408 waters (0–18 m).

409 **Variation:** The revised material showed three general outlines on the carapace shape. Between
410 males, a transversally subrectangular carapace shape was observed in 33% (three specimens) of
411 the revised material and comes from Sinaloa, a subovate shape was observed in 56% (five
412 specimens) of the material and comes from Guerrero and Oaxaca, and a subtrapezoidal shape in
413 11% (one specimen) comes from Oaxaca. In females, the subrectangular shape was observed in
414 11% (five specimens) of the material and comes from Sinaloa, the subovate shape in 85% (40
415 specimens) and comes from Guerrero and Oaxaca, and the subtrapezoidal shape in 2% (two
416 specimen) and comes from Oaxaca.

417 The subrectangular shape (Figs. 4A, 5A) is defined by a straight and notably projected margin of
418 the frontal lobes, a straight anterior margin in which the hepatic notch in males is notably deeper,
419 eroded, and extended over the carapace (Fig 4A, white arrow) but in females is less conspicuous
420 (Fig. 5A, black arrow), and in the male by a truncated and scarcely projected lateral lobes in
421 which the anterior portion in the male is concave (Fig. 4A, black arrow) but in the female is

422 straight. Instead, the subovate shape (Figs. 4E, I, 5D, G) is defined by an entire even margin
423 which is outlined by the slightly oblique and scarcely projected frontal lobes, the convex
424 anterolateral margin continues smoothly to the lateral margin forming a notably convex lobe
425 (Figs. 4E, I, black arrows) in which the hepatic notch in the males is shallow, slightly eroded and
426 less extended over the carapace (Fig. 4E, I, 5 D, G, white arrows). Meanwhile, the subtrapezoidal
427 shape is defined by the scarcely projected margin of the frontal lobes, which continues evenly
428 and smoothly to the straight anterolateral margin forming notably projected lateral lobes (Fig.
429 1D, 6A). In all the females, the margin of the frontal lobes and the eyes are not visible in dorsal
430 view and only a slight notch is visible (Figs. 5A, D, G, white arrows), because the frontal-dorsal
431 surface is more convex than in males, but if the carapace is placed so that the posterior margin
432 line of the carapace cannot be seen, then the general carapace outline looks like the males from
433 Guerrero or Oaxaca (v.g. Figs. 4E, I). Also, in frontal view, the convexity of the frontal-dorsal
434 surface allows a pair of inflated and only drawn lobes on the surface to be seen. The remarkably
435 convex frontal-dorsal surface which obscures the frontal margin and the eyes in dorsal view, was
436 observed in 16 specimens (15 females, one male), and the less convex shape was observed in 39
437 specimens (31 females, eight males). This notably convex shape was more frequent in ovigerous
438 females (10 specimens, 67%) than in non-ovigerous ones (five specimens, 33%). Despite the
439 variation in the shape of the carapace in both sexes, in all cases the CW/CL ratio is the same;
440 plus, the length measured from the notch of the margin of the frontal lobes to the external orbital
441 angle, and that of the external orbital angle to the posterior angle of the hepatic notch, are the
442 same.

443 Regarding the Mxp3, the ischiomerus external margin appears notably convex on its mid-distal
444 portion or slightly even throughout its length, and its inner margin could have a concave or

445 sinuous mid-distal portion; even so, the inner margin always has a blunt or slightly acute
446 projection (Figs. 4 Ca, Ga, Ka, 5Ca, Fa, Ia; black arrow), but its width/length ratio is constant in
447 all the outlines' variations. The carpus is conical, the main appearance variation is its length and
448 the convexity or straightness of its dorsal margin, but that is only related with the drawing
449 perspective (Figs. 4Cb, Gb, Kb, 5Cb, Fb, Ib), yet in all cases there is a projected ridge on the
450 internal surface which has a conspicuous tuft of setae. The propodus also looks variable in its
451 width/length ratio and in its more acute or rounded distal margin, nevertheless that is the result of
452 the way in which the piece was mounted; despite that, its proximal ventral margin always forms
453 a straight angle in which the dactylus is jointed (Figs. 4Cc, Gc, Kc, 5Cc, Fc, Ic). Finally, the
454 dactylus shows two closely related outlines, one subspatulated and the other suboblong, the first
455 has a more expanded distal portion instead of a narrow shape as in the latter; nevertheless, its
456 distal margin always slightly overreaches the propodus (Figs. 4Cd, Gd, Kd, 5Cd, Fd, Id).

457 Variation in the ornamentation of the chelae fingers is observed. Between males, the cutting edge
458 of the movable finger has two to three proximal blunt or acute teeth (Figs. 4B, F, J, black
459 arrows), the medial tooth is simple (Figs. 4B, J, white arrow) or bicuspid (Fig. F, white arrow),
460 and the subdistal projection is acute (Figs. 4B, F, white dashed arrow) or blunt (Fig. 4J, white
461 dashed arrow); the fixed finger has six to nine blunt (Fig. 5B) or acute (Fig. 5F, J) teeth, and the
462 middle or more conspicuous tooth is always bicuspid (Figs. 4B, F, J, black arrow). Between
463 females, the movable finger shows two to three acute teeth (Fig. 5B, E, H, black arrow), an acute
464 (Figs. 5B, E, white arrow) or blunt (Fig. 5H, white arrow) medial tooth, and a blunt subdistal
465 projection (Figs. 5B, E, H, white dashed arrow); the fixed finger has four to thirteen teeth with a
466 bicuspid blunt medial tooth (Fig. B, E, black arrow) or a simple acute one (Fig. H, black arrow).

467 Only one specimen (DECA-1172) has different size chelae and a different teething pattern on the
468 cutting edge of the fixed finger (Fig. 5J, K).

469 The first gonopod of the males shows variation in the degree of curvature and the amount of the
470 distal portion that is curved, and also in the general outline shape of the gonopod tip, but may be
471 similar in different stages of development. In this sense, the general appearance in the abdominal
472 view, of males from Sinaloa and Oaxaca is more similar because the external and internal
473 margins are sinuous (Figs. 4D, L), the curvature degree is approximately 90° (Fig. 4D) and 75°
474 (Fig. 4L) respectively, the tip of the external margin is truncated (Figs. 4De-f, Le-f; white arrow),
475 and the ventral margin of the tip has a blunt projection (Figs. 4De, Le; black arrow); while in that
476 of Guerrero, the external and internal margins are less sinuous and the curvature degree is
477 approximately 65° (Fig. 4H), the tip of the external margin is convex (Fig. 4He-f; white arrow),
478 and the ventral margin of the tip has a pointed projection (Fig. 4He; black arrow). Also, in sternal
479 view, the ventral process shape of the internal margin tip is variable, in males from Sinaloa it is
480 obtuse (Fig. 4D-f; black arrow), while in those from Guerrero it is convex (Fig. 4H-f; black
481 arrow) and those from Oaxaca is oblique (Fig. 4L-f; black arrow), but this is variable also
482 between the sizes of the crabs.

483 **Remarks:** All the biological material examined shows phenotypic variation, particularly
484 between the individuals from the type locality in Mazatlan with respect to those of Guerrero and
485 Oaxaca, but molecular evidence show no differentiation. Now with the description of the male
486 morphology it is possible to differentiate *Holothuriophilus trapeziformis* from *H. pacificus* with
487 certainty because the carapace could be subrectangular (Fig. 4A, 5A), suboval (Fig. 4E, I, 5D, G)
488 or subtrapezoidal (Fig. 1A, D, 2A, 6A) in the former but it is subcuadrangular in the latter (Fig.
489 6E). *H. trapeziformis* has the Mxp3 dactylus with its distal portion notably expanded, the

490 external distal margin slightly truncated, and the flagellum of the exopod is long and robust
491 (Figs. 6B, J, K, 7A); but in *H. pacificus* the distal margin is rounded and the flagellum of the
492 exopod is long and slender (Figs. 6F, 7D). The first gonopod of *H. trapeziformis* has a more
493 sinuous lateral margins with a larger distal portion curved outwards with abundant setae (Fig.
494 7C); however, in *H. pacificus* it is straight with only the distal portion slightly curved outwards,
495 and with less abundant setae (Fig. 7F). The abdomen of *H. trapeziformis*, in males, is
496 subtriangular with lateral margins narrowing from the fourth to the sixth somite, the third somite
497 has notably convex lateral margins, the sixth somite has notably concave lateral margins, and the
498 telson is subrounded and wider than long (Fig. 7B); yet in *H. pacificus* it is triangular, the lateral
499 margins are almost straight, the third and sixth somite lateral margins are concave, and the telson
500 is subtriangular and longer than wide (Fig. 7E). In the case of *Holothuriophilus trapeziformis*
501 adult ovigerous and non-ovigerous females, the abdomen is suboval and wider than long, the first
502 somite has convex lateral margins, the second somite has a sinuous distal margins, the third
503 somite has an oblique and downward lateral margins, the sixth somite has oblique and outward
504 lateral margins, and the telson has a length to width ratio ca. 0.2 (Fig. 6D); instead in *H.*
505 *pacificus* it is suboval and longer than wide, the first somite has concave lateral margins, the
506 second somite has an almost straight distal margins, the third somite has oblique and upwards
507 lateral margins, the sixth somite has convex lateral margins, and the telson has a length to width
508 ratio ca. 0.3 (Fig. 6H).

509 **Distribution and ecological comments:** The present study allows us to increase the previous
510 known distribution range from Punta Tiburon, Sinaloa to playa Las Gatas, Guerrero, to the south,
511 615 km to playa Tejon, Oaxaca. We found crabs in the coelom cavity and near the cloaca of the
512 host, as mentioned by Manning (1993), Campos, Peláez-Zárate & Solís-Marín (2012) and

513 Honey-Escandón & Solís-Marín (2018) and, for the first time, it is registered within the intestine
514 (Fig. 1G).

515 *Holothuria (Halodeima) inornata* is distributed throughout the Tropical Eastern Pacific from the
516 Gulf of California, Mexico to Ecuador, and in the temperate island Lobos de Afuera, Peru
517 (Prieto-Rios et al. 2014; Honey-Escandón & Solís-Marín 2018). It also, represents an important
518 fishery resource throughout its distribution range (Santos-Beltrán & Salazar-Silva 2011), yet
519 there are no records for *Holothuriophilus trapeziformis* outside the Pacific coast of Mexico.

520 **Molecular approach**

521 **DNA Barcodes**

522 From the 56 examined crabs (Table S1), 51 were processed. The number of base pairs was
523 between 549 bp and 648 bp for 37 specimens with a sole Barcode Index Number (BIN;
524 Ratnasingham & Hebert 2013) in the BOLD database: ADE9974. Of those, 35 produced a high-
525 quality barcode. The 14 crabs that could not be amplified correspond to old museum material and
526 to recent collections that are not fixed according to the Elías-Gutiérrez et al. (2018) protocol. A
527 BLAST query in GenBank confirmed our sequences to belong to a brachyuran lineage. Finally,
528 in the case of the hosts, none could be amplified.

529 **Phylogeny and distance analysis**

530 The best nucleotide substitution model according to AIC and BIC criterion was General Time
531 Reversible under a gamma distribution (GTR+G) model (Nei & Kumar 2000). The Maximum-
532 Likelihood (ML) distance method under the selected model delimited the 37 sequences of
533 *Holothuriophilus trapeziformis* from the dataset (DS-PINMX1HT) in a single cluster; however,
534 two sub-groups are defined, one for Sinaloa (northern) and the other for Guerrero and Oaxaca
535 (southern). These two clusters are well separated from the sister group, *H. pacificus*, in the

536 maximum likelihood tree (ML) as can be seen in figure 8, with a 12 to 14% of divergence among
537 all specimens. *Holothuriophilus* is also related to the *Calyptraeotheres* clade, but far from other
538 species (Fig. 8) with an interspecific divergence ranging from 12 to 19%.

539 **Intraspecific DNA polymorphisms and historical demography**

540 Although the *Holothuriophilus trapeziformis* clade shows two well differentiated groups, its
541 intraspecific divergences ranged from 0 to 2.2%. This is congruent with the BOLD distance
542 summary analyses which show an average distance of 0.73% and a maximum of 2.27% for
543 sequences with more than 500bp. For *Holothuriophilus trapeziformis* from the Pacific coast of
544 Mexico we identified 34 nucleotide substitutions (28 transitions, 6 transversions), and 33
545 polymorphic sites (14 parsimony informative sites and 19 singleton variables) that defined 22
546 unique COI haplotypes with a moderate mean number of nucleotide differences between pairs
547 ($k= 3.775$), and total genetic diversity estimations indicate a high haplotype diversity ($Hd =$
548 0.914) but a moderated nucleotide diversity ($\pi= 0.007$) (Table 1). Within-regions the haplotype
549 diversity was high in all localities (ranging from 0.874–0.964), and the nucleotide diversity
550 shows an increment along the considered latitudinal gradient from south to north (Oaxaca and
551 Guerrero with 0.003 and 0.006, respectively, and Sinaloa with 0.009) (Table 1).

552 Of the 22 haplotypes (Table 2), the H3 is the most abundant and is present in all sites.

553 Nevertheless, two haplogroups were well defined (Fig. 9); one haplogroup is formed by 18
554 haplotype related to Guerrero and Oaxaca localities from which H3 is most frequent, and the
555 other haplogroup is represented by four exclusive haplotypes from Sinaloa (H1, H2, H4, H5).

556 A genetic differentiation among sample sites was demonstrated by pairwise Φ_{ST} values. A low
557 value was observed between Guerrero vs. Oaxaca ($\Phi_{ST}= 0.06286$, $p= 0.027$), while a high value

558 was shown between Sinaloa vs. Guerrero ($\Phi_{ST} = 0.44434$, $p = 0.004$) and Sinaloa vs. Oaxaca
559 ($\Phi_{ST} = 0.57864$, $p \leq 0.001$).

560 SAMOVA results indicated that genetic differentiation was better when considering two groups
561 ($k = 2$; Group 1: Sinaloa, Group 2: Guerrero-Oaxaca) because 53% of the variance is explained
562 (Table 3), in contrast to 44% of the variation when considering a single group ($k = 1$; Group 1:
563 Sinaloa-Guerrero-Oaxaca) (Table 4). This result confirmed the groups previously defined by the
564 haplotype network as haplogroup A (Guerrero-Oaxaca) and haplogroup B (Sinaloa) with a $\Phi_{CT} =$
565 0.53 ($p \leq 0.001$) as shown in table 3. The Mantel test showed significant relationships among
566 these variables ($r = 0.604$; $p < 0.0001$) suggesting patterns of isolation by distance.

567 Under the coalescent method, the overall *Holothuriophilus trapeziformis* mismatch distribution
568 indicates a significant ragged unimodal distribution (Fig. 10A; $r = 0.07780$, $p = 0.0280$; $R_2 =$
569 0.11407, $p = 0.0000$). At the regional scale, in Sinaloa a multimodal distribution was observed
570 (Fig. 10B; $r = 0.22104$, $p = 0.57700$; $R_2 = 0.20112$, $p = 0.0260$), whereas in Guerrero it was
571 bimodal (Fig. 10C; $r = 0.15286$, $p = 0.200800$, $R_2 = 0.18034$, $p = 0.0260$), and in Oaxaca it was
572 unimodal (Fig. 10D; $r = 0.08442$, $p = 0.23400$; $R_2 = 0.12867$, $p = 0.00600$).

573 The neutrality test of Tajima's D for the overall *H. trapeziformis* was negative and significant
574 (Tajima's D = -1.83464, $p = 0.01100$), pointing to a population expansion. When Fu's (Fs) is
575 taken into account, all the population levels were negative and significant, also indicating an
576 expansion. Finally, the raggedness index (r) indicates a population growth, as its values were low
577 but not significant in all the population levels, as well as the R_2 that indicated an expansion
578 model in all cases (Table 1). We preferred to use the Tajima's D and the R_2 estimations, instead
579 of Fu's (Fs), because of the small sample size, and because it is known that these parameters are

580 particularly recommended when recombination levels are unknown (Ramos-Onsins & Rozas,
581 2002; Ramírez-Soriano et al., 2008)

582 **Discussion**

583 We detect high variability in some of the most external features in *Holothuriophilus*
584 *trapeziformis*. The general body appearance of the northern specimens from the type locality
585 (Mazatlan, Sinaloa) is more robust and eroded with shorter pereopod segments than those of the
586 southern localities (Guerrero and Oaxaca). Taking into account that for pinnotherids taxonomy a
587 crucial goal is to provide a complete description with detailed illustrations of common and
588 unusual structures (Derby & Antema 1980; Ahyong, Komai & Watanabe 2012; Salgado-
589 Barragan 2015) for comparative purposes, then the selected material in this research is 2 mm less
590 than the female described by Bürger (1895) and 0.3 mm greater than the female lectotype
591 described by Ahyong & Ng (2007). Therefore, the morphological variation of the females could
592 be contrasted with the available illustrations, and the description of the species was completed
593 with the morphology of the male. In the available female illustrations, a presumable specimen
594 from the type locality shows a subrounded carapace shape (Bürger, 1895: 380–381, pl. 9, fig. 26,
595 plate 10, fig. 25; CW = 14 mm, CL = 10 mm) and the lectotype, also from the type locality,
596 shows it as subovate (Ahyong & Ng 2007: 214, Fig. 20A; CW = 7.7 mm, CL = 4.8 mm; in the
597 present document see Fig. 6I), but another from Guerrero has a subtrapezoidal shape (Campos,
598 Peláez-Zárate & Solís-Marín 2012: 60, fig. 2B; CW = 9.1 mm, CL = 5.2 mm). In the revised
599 females, variations of the carapace shape are due to the projection of the lateral lobes and by the
600 convexity of the front-dorsal surface; the revised males in contrast with the females, have less
601 expanded and projected lateral lobes, a more pilose pterigostomian region, and slightly less
602 abundant setae on the pereopods. Additionally, the first gonopod of the males shows a different

603 appearance in the three geographic regions, but that from Sinaloa is more similar to that of
604 Oaxaca in its general shape, setae pattern, and degree of curvature of the apical portion, than to
605 that from Guerrero (see Fig. 4D, H, L) when the most developed stage is considered; however,
606 that can be variable within the same locality. In contrast, the second gonopod (Fig. 2F) shows no
607 differences between all the examined males. Variations in the Mxp3 between sexes is common,
608 but setae pattern and abundance correspond to that shown by Campos, Peláez-Zárate & Solís-
609 Marín (2012; Fig. 6K). We believe that the state of development and the position in which the
610 specimen was observed and drawn are the primary causes of the differences between the
611 available illustrations.

612 Despite the facts mentioned above, we can conclude that *Holothuriophilus trapeziformis* is
613 different from *H. pacificus* not only by the absence of a space when the fingers are closed (see
614 Figs. 6C, G) as pointed out by Campos, Peláez-Zárate & Solís-Marín (2012), but also because *H.*
615 *pacificus* does not have a convex mid-distal projection on the cutting edge of the mobile finger
616 (Fig. G) as *H. trapeziformis* does (Fig. 4B, F, J, 5B, E, H; dotted arrow). Additionally, these
617 species can be separated by the shape of the abdomen of both sexes (Figs. 6D, H, 7B, E), and by
618 the structure of male's first gonopod (Figs. 7C, F). Also, *H. trapeziformis* has a granulated
619 ventral surface on the palm of the chelae, mostly on larger sized mature crabs (Fig. 7 C; dashed
620 arrow); that condition is not documented for *H. pacificus* in Garth (1957; fig. 7G) and its
621 synonyms (= *Leucosia pacifica* Poepig, 1983 = *Pinnaxodes silvestrii* (Nobili, 1901) = *Pinnaxodes*
622 *meinerti* Rathbun, 1904).

623 Regarding the molecular approach, *Holothuriophilus trapeziformis* did not have previous genetic
624 information. The success of the COI gene amplification of *Holothuriophilus trapeziformis* was
625 accomplished after the implementation of the chilled ethanol preservation protocol suggested by

626 Elías-Gutiérrez et al. (2018). Due to the thickness of the cuticle, we decide the injection of
627 ethanol inside the body of the crabs through the joints of the armature, as well as the use of
628 zooplankton primers (Prosser, Martínez-Arce & Elías-Gutiérrez 2013) instead of Folmer or other
629 generic primers. With these improvements, we obtained the amplification of 72% of the total
630 sample and a total of 69% sequencing success on a group that is considered difficult to work
631 with COI genes (Mantellato et al. 2016) and this allowed to us to obtain some basic genetic
632 parameters (Table 8). Those results allowed us to confirm the taxonomic status of
633 *Holothuriophilus trapeziformis* as a valid species since the different analyses based on the COI
634 gene fragment (vg. Barcode BIN, IDtree, and Maximum likelihood phylogenetic topology)
635 indicated a divergence ranging from 12 to 14% against *H. pacificus*. These values are above the
636 3% threshold proposed by Hebert et al. (2003) as a tool to recognize taxonomic units. They also
637 fall into the pairwise distance ranges proposed for crustacean congeners (1.5% to 3.3%, average=
638 2.5%; Lefébure et al. 2006) and Decapoda congeners (4.92% to 31.39 %, average= 17.16%;
639 Costa et al. 2007), although these values are slightly lower, they fit within the ranges for
640 pinnotherids (15.5% to 24.6%, average= 18.3%; Ocampo et al. 2013). Our Maximum-Likelihood
641 tree agrees with that of Palacios-Theil, Cuesta & Felder (2016) in regards with the association of
642 the genus *Holothuriophilus* and *Calyptraeotheres*.

643 Phenotype variation is a result of a plastic response to different environmental pressures,
644 particularly when the species shows a wide distribution in heterogeneous or geographically
645 isolated environments (Hurtado, Mateos & Santamaria 2010; Rossi & Mantelatto 2013); also,
646 recent or historical processes that limit the flow of genes determine a genetic structure in the
647 populations of the species, but it has been considered that in the marine province the species
648 exhibit low levels of differentiation even if there are environmental barriers (Wares, Gaines &

649 Cunningham 2001; Avise 2009). However, in brachyuran crabs, much evidence has been argued
650 against that, principally because of the particularities of the geographic areas, the habitat
651 peculiarities, and by the species life history as has been documented for grapsids (Cassone &
652 Boulding 2006), ocypodids (Laurenzano, Mantelato & Schubart 2013), pinnotherids (Ocampo et
653 al. 2013), sesarmids (Zhou et al. 2015), and varunids (Zhang et al. 2017).

654 Pinnotherid crabs are known to have a complex life cycle and ample time for their development
655 lasting from 26 to 30 days (Bousquette 1980; Hamel, Ng & Mercier 1999; Ocampo et al. 2011),
656 which allows them to maintain connectivity between populations throughout their geographical
657 distribution range (Ocampo et al. 2013); however, in this case, connectivity through larval
658 dispersal may be more restricted due to their symbiotic behavior and the specificity of the
659 relationship with their host than due to other environmental factors (Haines, Edmunds & Pewsey
660 1994; Hamel, Ng & Mercier 1999; Ocampo et al. 2012, 2013; Guilherme, Brustolin & de Bueno
661 2015; Becker & Türkay 2017). *Holothuriophilus trapeziformis* has been considered as an
662 endobiotic parasite of their host since its description (Nauck 1880), but no other related
663 reference confirms that type of interaction (Bürger 1895; De Man 1887; Ng & Manning 2003;
664 Ahyong & Ng 2007; Campos, Peláez-Zárate & Solís-Marín 2012). Of the thirteen pinnotherids
665 known to develop this endobiotic way of life, living near the respiratory trees, the coelomic
666 cavity, or the posterior part of the digestive gut, and could or could not cause detrimental effects
667 (Hamel, Ng & Mercier 1999; Ng & Manning 2003); only the life cycle of *Holotheres haling* has
668 been described in detail (Hamel, Ng & Mercier, 1999). In contrast, the life cycle of
669 *Holothuriophilus trapeziformis* is still unknown. As a starting point to generate information
670 about it, we only collected the holothurian species *Holothuria (Halodeima) inornata* in
671 accordance to Honey-Escandón & Solís-Marín (2018), but some other holothurians from the

672 South Pacific coast of were also examined in search of the symbiont, with no success. Thus, we
673 found the crab inhabiting in a membranaceous cyst through the coelomic cavity and inside of the
674 gut, and never found more than one crab together.

675 Besides the cyst cavity wound produced by the crab on the cloacal internal wall, we also found
676 some crabs with pieces of the respiratory tree in their pincers and inside their buccal cavity.

677 *Holothuriophilus trapeziformis* has spoon-tipped fingers but not much is known about the precise
678 function of this kind of condition, but it is associated with feeding on detritus, scooping up
679 mucus from corals, picking up soft foods, scraping off encrusting algae, effective gripping of
680 filamentous algae, or scraping epilithic algae off coral rock (Davie, Guinot & Ng 2015);
681 however, there is no information on this respect for pinnotherids with this condition. It is
682 necessary to examine the stomach contents to corroborate that the crab feeds only on the host
683 tissue or also on detritus of the intestine, and to evaluate in some way the physiological damage
684 produced in the host to determine with certainty if the agonistic interaction corresponds to a
685 parasitism or a commensalism.

686 With this context, the *Holothuriophilus trapeziformis* morphological variation and significant
687 genetic differentiation through its distribution range was indicated and supported by the
688 haplotype network, the Φ_{ST} index, SAMOVA and Mantel test, mainly in the distinction between
689 the northern and southern forms. But, the range of the intraspecific distance values corresponds
690 to the thresholds proposed for crustaceans (Lefébure et al. 2006), for decapods (Costa et al.
691 2007), and for pinnotherids (Ocampo et al. 2013) to maintain the intraspecific delimitation. In
692 addition, a sudden expansion of population growth was evidenced by a gene flow from the south
693 to the north, due to the overall high haplotype and low nucleotide diversity detected with 22
694 haplotypes in 37 individuals from which all the haplotypes derived from a possible ancestral

695 haplotype (H3) in Oaxaca. The overall unimodal mismatch distribution displayed, and the
696 negative and significant results of the neutrality Tajima's (D) and Fu's (Fs) test, support that
697 scenario.

698 Nevertheless, the morphological difference and the pairwise genetic distance observed in Sinaloa
699 could represent a process of differentiation since the mismatch distribution there shows a
700 multimodal form that is statistically not significant (Fig. 10B; $r = 0.22104$, $p = 0.57700$; $R^2 =$
701 0.20112 , $p = 0.0260$). Sample size is significant and correlated with the number of haplotypes
702 (Cassone & Boulding 2006) and probably has an effect over the mismatch distributions.

703 Additionally, in this northern area the presence of the Thermocline Cabo Corrientes Dome
704 (Gómez-Valdivia, Parés-Sierra & Flores-Morales 2015) probably acts as a physical barrier to the
705 flow of genes from the south. Northern specimens are genetically and morphologically different
706 to those of the southern Mexico, but correspond with the model of isolation by distance, in which
707 the differences between populations are due to limited gene flow because of a restricted
708 geographical dispersion, the near-surface marine circulation patterns, the discontinuity of
709 habitats, and the frequency of sexual reproduction. This kind of situation has been demonstrated
710 for other decapods with a complex life cycle (Rossi & Mantelatto 2013).

711 Considering the *Holothuriophilus trapeziformis*' way of life and its relationship with its host, the
712 environmental pressures determining the genetic connectivity correspond to geographical
713 barriers (extended estuarine areas and wide sandy beaches between the rocky shores) and
714 oceanographic processes (Mexican Coastal Current, Thermocline of Cabo Corrientes Dome, and
715 Thermocline of the Tehuantepec Bowl) through the Pacific coast of Mexico (Hurtado et al. 2007;
716 Paz-García et al. 2012; Gómez-Valdivia, Parés-Sierra & Flores-Morales 2015), which influence
717 the gene flow. This is important because the host, *Holothuria (Halodeima) inornata*, shows a

718 wide distribution range across the subtropical American Pacific coast, with two well defined
719 genetic populations: A Mexican one—Gulf of California to Oaxaca— and a Panamic one—from
720 Chiapas, Mexico to Peru, inhabiting rocky shores (Prieto-Rios et al. 2014). Despite the
721 specificity of the association with *Holothuria (H.) inornata* (Honey-Escandón & Solís-Marín
722 2018) no records of *Holothuriophilus trapeziformis* south to Oaxaca are known. Until now, and
723 with all the evidence presented here, *Holothuriophilus trapeziformis* has the status of endemic
724 species of Mexico; therefore, in order to establish that status, it is necessary to confirm the
725 presence or absence of the species in the distribution range of *Holothuria (H.) inornata* outside
726 of Mexico.

727 We can conclude that the taxonomic status of *Holothuriophilus trapeziformis* is now completed,
728 recognized based on the morphology of both sexes, and the genetic and demographic historical
729 analyses, that confirm the taxonomic status of all the revised material as the same species by
730 linking all the sequenced material with a new DNA barcode (BOLD:ADE9974) different from
731 that of *H. pacificus* (BIN, BOLD: ABV9743; boldsystems.org). We also suggest that
732 morphological plasticity is the result of an isolation by distance experienced by the individuals in
733 the considered regions after a sudden population expansion throughout their life history. In spite
734 of that, however, the specialized relationship with their host, the restricted habitat in which they
735 live, and local environmental barriers are perhaps the main forces that have caused this plasticity.

736 **Acknowledgements**

737 We are grateful to the Chetumal Node of the Mexican Barcode of Life (MEXBOLD) for support
738 for the genetic analysis, in particular to Alma Estrella García-Morales who assisted with the
739 DNA process of the biological samples. To J. Rolando Bastida-Zavala for the access to the
740 collection material of Laboratorio de Sistemática de Invertebrados Marinos (LABSIM) from

741 Universidad del Mar. To José Luis Villalobos-Hiriart and Fernando Álvarez-Noguera for the
742 access to the collection material of the Colección Nacional de Crustáceos (CNCR) del Instituto
743 de Biología de la Universidad Nacional Autónoma de México. To Virgilio Antonio Pérez and
744 staff from Buceo Huatulco for their support during the field work. ME-G and MSGM recognize
745 the high authorities of the Mexican government for their effort to smother all aspects of science
746 progressively, particularly in the biodiversity conservation, as a motivation to produce and
747 conclude this work. We will continue training human resources in this area as a commitment to
748 Mexico and our planet.

749 **References**

- 750 **Adensamer T.** 1887. Revision der Pinnotheriden in der Sammlung des K. K. Naturhistorischen
751 Hofmuseums in Wien. *Annalen des K.K. Naturhistorischen Hofmuseums* 12:105–110.
- 752 **Ahyong ST, Ng PKL.** 2007. The pinnotherid type material of Semper (1880), Nauck (1880) and
753 Bürger (1895) (Crustacea: Decapoda: Brachyura). *Raffles Bulletin of Zoology Supplement*
754 16:191–226.
- 755 **Ahyong ST, Komai T, Watanabe T.** 2012. First *Viridotheres* Manning, 1996, from Japan, with
756 a key to the species (Decapoda, Brachyura, Pinnotheridae). In: Komatsu H, Okuno J,
757 Fukuoka K, eds. *Studies on Eumalacostraca: A Homage to Masatsune Takeda,*
758 *Crustaceana Monographs* 17:35–47 https://doi.org/10.1163/9789004202894_003
- 759 **Awise JC.** 2009. Phylogeography: retrospect and prospect. *Journal of Biogeography* 36:3–15
760 <https://doi.org/10.1111/j.1365-2699.2008.02032.x>
- 761 **Balss H.** 1957. Decapoda. In: Bronns GH, ed. *Klassen und Ordnungen des Tierreichs.* Fünfter
762 Band 5, 1 Abteilung, 7 Buch, 12 Lieferung. pp. 1505–1672.

- 763 **Becker C, Türkay M.** 2017. Host specificity and feeding in European pea crabs (Brachyura,
764 Pinnotheridae). *Crustaceana* 90(7–10):819–844 [https://doi.org/10.1163/15685403-](https://doi.org/10.1163/15685403-00003661)
765 [00003661](https://doi.org/10.1163/15685403-00003661)
- 766 **Brandão M, Freire AS, Burton RS.** 2016. Estimating diversity of crabs (Decapoda: Brachyura)
767 in a no-take marine protected area of the SW Atlantic coast through DNA barcoding of
768 larva. *Systematics and Biodiversity* 14(3):288–302
769 <https://doi.org/10.1080/14772000.2016.1140245>
- 770 **Bousquette GD.** 1980. The larval development of *Pinnixa longipes* (Lockington, 1877)
771 (Brachyura: Pinnotheridae) reared in the laboratory. *Biological Bulletin* 159:592–605
772 <https://doi.org/10.2307/1540825>
- 773 **Bürger O.** 1895. Ein Beitrag zur Kenntniss der Pinnotherinen. *Zoologische Jahrbücher,*
774 *Abtheilung für Systematik, Geographie und Biologie der Thiere* 8:361–390.
- 775 **Campos E, Díaz V, Gamboa-Contreras JA.** 1998. Notes on distribution and taxonomy of five
776 poorly known species of pinnotherid crabs from the eastern Pacific (Crustacea: Brachyura:
777 Pinnotheridae). *Proceedings of the Biological Society of Washington* 111:372–381.
- 778 **Campos E, Peláez-Zárate V, Solís-Marín FA.** 2012. Rediscovery, host and systematics of
779 *Holothuriophilus trapeziformis* Nauck, 1880 (Crustacea, Brachyura, Pinnotheridae).
780 *Zootaxa* 3528:57–62 <https://doi.org/10.11646/zootaxa.3528.1.4>
- 781 **Caso ME.** 1958. Contribución al conocimiento de los holoturoideos de México. III. Algunas
782 especies de holoturoideos litorales de la costa Pacífica de México. *Anales del Instituto de*
783 *Biología, Universidad Nacional Autónoma de México* 28:309–338.

- 784 **Caso ME.** 1964. Contribución al conocimiento de los holoturoideos de México. Descripción de
785 una n. sp. de *Holothuria* de un nuevo subgénero (*Paraholothuria* N. SG.). *Anales del*
786 *Instituto de Biología, Universidad Nacional Autónoma de México* 34(1–2):367–380.
- 787 **Caso ME.** 1965. Estudio sobre Equinodermos de México. Contribución al conocimiento de los
788 holoturoideos de Zihuatanejo y de la Isla de Ixtapa (primera parte). *Anales del Instituto de*
789 *Biología, Universidad Nacional Autónoma de México* 36:253–291.
- 790 **Cassone JB, Boulding GE.** 2006. Genetic structure and phylogeography of the lined shore crab,
791 *Pachygrapsus crassipes*, along the northeastern and western Pacific coast. *Marine Biology*
792 149:213–226 <https://doi.org/10.1007/s00227-005-0197-9>
- 793 **Clement, M, Snell Q, Walker P, Posada D, Crandall K.** 2002. TCS: Estimating gene
794 genealogies. *Parallel and Distributed Processing Symposium, International Proceedings*
795 2:184 <https://doi.org/10.1109/IPDPS.2002.1016585>
- 796 **Costa FO, De Waard JR, Boutillier J, Ratnasingham S, Dooh RT, Hajibabaei M, Hebert**
797 **PDN.** 2007. Biological identification through DNA barcodes: the case of the Crustacea.
798 *Canadian Journal of Fisheries and Aquatic Science* 64:272–295
799 <https://doi.org/10.1139/f07-008>
- 800 **Darriba D, Taboada GL, Doallo R, Posada D.** 2011. jModelTest 2: more models, new
801 heuristics and parallel computing. *Nature Methods* 9(8):772
802 <https://doi.org/10.1038/nmeth.2109>
- 803 **Davie PJF, Guinot D, Ng PKL.** 2015. Anatomy and functional morphology of Brachyura. In:
804 Castro, P., Davie, P.J.F., Guinot, D., Schram, F. & von Vaupel Klein, C. (Eds.) *Treatise on*
805 *zoology – anatomy, taxonomy, biology- The crustaceae, complementary to the volumes*
806 *translated from the French of the Traité de Zoologie, 9 (C) (I), Decapoda: Brachyura*

- 807 (Part 1), Koninklijke Brill NV, Leiden, pp. 11–163
808 https://doi.org/10.1163/9789004190832_004
- 809 **Derby CD, Antema J.** 1980. Induced host odor attraction in the pea crab *Pinnotheres*
810 *maculatus*. *Biological Bulletin* 158:26–33 <https://doi.org/10.2307/1540755>
- 811 **De Man JG.** 1887. Uebersicht der Indo-pacifischen Arten der Gattung *Sesarma* Say, nebst einer
812 Kritik der von W. Hess und E. Nauck in den Jahren 1865 und 1880 beschriebenen
813 Decapoden. *Zoologische Jahrbücher. Abteilung für Systematik, Geographie und Biologie*
814 *der Tier* 2:639–722.
- 815 **Dupanloup I, Schneider S, Excoffier L.** 2002. A simulated annealing approach to define the
816 genetic structure of populations. *Molecular Ecology* 11:2571–2581
817 <https://doi.org/10.1046/j.1365-294X.2002.01650.x>
- 818 **Elías-Gutiérrez M, Valdez-Moreno M, Topan J, Young MR, Cohulo-Colli JA.** 2018.
819 Improved protocols to accelerate the assembly of DNA barcode reference libraries for
820 freshwater zooplankton. *Ecology and Evolution* 8:3002–3018
821 <https://doi.org/10.1002/ece3.3742>
- 822 **Excoffier L, Lischer H.** 2015. Arlequin ver 3.5 An integrated software package for population
823 genetics data analysis. Available from: <http://cmpg.unibe.ch/software/arlequin35> (accessed
824 5 January 2019)
- 825 **Garth SJ.** 1957. Reports of the Lund University Chile Expedition 1948–49, 29, The crustacea
826 decapoda brachyura of Chile. *Lunds Universitets Årsskrift*. N.F. Avd. 2. Bd. 53. Nr. 7:1–
827 134.
- 828 **Garm A, Watling L.** 2013. The crustacean integument: setae, setules, and other ornamentation.
829 In: Watling, L. & Thiel, M. (Eds.) *Functional morphology and diversity. The natural*

- 830 *history of crustacean series*, 1. Oxford University Press, Oxford, pp:167–198
- 831 <https://doi.org/10.1093/acprof:osobl/9780195398038.003.0006>
- 832 **Gómez-Valdivia F, Parés-Sierra A, Flores-Morales AL.** 2015. The Mexican Coastal Current:
833 A subsurface seasonal bridge that connects the tropical and subtropical Northeastern
834 Pacific. *Continental Shelf Research* 110:100–107 <https://doi.org/10.1016/j.csr.2015.10.010>
- 835 **Guilherme PDB, Brustolin MC, de Bueno ML.** 2015. Distribution of ectosymbiont crabs and
836 their sand dollar host in a subtropical estuarine sandflat. *International Journal of Tropical*
837 *Biology, Revista de Biología Tropical* 63(2):209–220.
- 838 **Haines CMC, Edmunds M, Pewsey AR.** 1994. The pea crab, *Pinnotheres pisum* (Linnaeus
839 1767), and its association with the common mussel, *Mytilus edulis* (Linnaeus, 1758), in the
840 Solent (U.K.). *Journal of Shellfish Research* 13:5–10.
- 841 **Hajibabaei M, De Waard JR, Ivanova NV, Ratnasingham S, Dooh RT, Kirk SL, Mackie**
842 **PM, Hebert PDN.** 2005. Critical factors for assembling a high volume of DNA barcodes.
843 *Philosophical Transactions of The Royal Society of London B Biological Science*
844 360:1959–1967 <https://doi.org/10.1098/rstb.2005.1727>
- 845 **Hajibabaei M, Singer GAC, Hebert PDN, Hickey DA.** 2007. DNA barcoding: how it
846 complements taxonomy, molecular phylogenetics and population genetics. *TRENDS in*
847 *Genetics* 23(4):167–172 <https://doi.org/10.1016/j.tig.2007.02.001>
- 848 **Hall TA.** 1999. BioEdit: a user-friendly biological sequence alignment editor and analysis
849 program for Windows 95/98/NT. *Nucleic Acids Symposium Series* 41:95–98.
- 850 **Hamel JF, Ng PKL, Mercier A.** 1999. Life cycle of the pea crab *Pinnotheres halingi* sp. nov.,
851 and obligate symbiont of the sea cucumber *Holothuria scabra* Jaeger. *Ophelia* 50(3):149–
852 175 <https://doi.org/10.1080/00785326.1999.10409393>

- 853 **Harpending H.** 1994. Signature of ancient population growth in a low resolution mitochondrial
854 DNA mismatch distribution. *Human Biology* 66:591–600.
- 855 **Harpending H, Sherry ST, Rogers AR, Stoneking M.** 1993. The genetic structure of ancient
856 human populations. *Current Anthropology* 34:483–496 <https://doi.org/10.1086/204195>
- 857 **Hartl DL, Clark AG.** 1997. *Principles of population genetics*. Sinauer Associates, Inc.
858 Sunderland, Massachusetts, 542 pp.
- 859 **Hebert PND, Cywinska A, Ball SL, De Waard JR.** 2003. Biological identification through
860 DNA Barcodes. *Proceedings of the Royal Society of London. Series B, Biological Science*
861 270 (1512):313–321 <https://doi.org/10.1098/rspb.2002.2218>
- 862 **Honey-Escandón M, Solís-Marín FA.** 2018. A revision of *Holoturia* (*Halodeima*) *kefersteinii*
863 (Selenka, 1867) and the revival of *Holothuria inornata* Semper, 1868 from sea cucumbers
864 collected in Mexico and Central America. *Zootaxa* 4377(2):151–77
865 <https://doi.org/10.11646/zootaxa.4377.2.1>
- 866 **Hurtado LA, Frey M, Guebe P, Pfeiler E, Markow TA.** 2007. Geographical subdivision,
867 demographic history and gene flow in two sympatric species of intertidal snails, *Nerita*
868 *scabricosta* and *Nerita funiculata*, from the tropical eastern Pacific. *Marine Biology*
869 151:1863–1873 <https://doi.org/10.1007/s00227-007-0620-5>
- 870 **Hurtado LA, Mateos M, Santamaria CA.** 2010. Phylogeography of supralittoral rocky
871 intertidal *Ligia* isopods in the Pacific region from Central California to Central Mexico.
872 *PLoS ONE* 5(7):e11633 <https://doi.org/10.1371/journal.pone.0011633>
- 873 **Ivanova NV, De Waard JR, Hebert, PDN.** 2006. An inexpensive, automation-friendly protocol
874 for recovering high-quality DNA. *Molecular Ecology Notes* 6:998-1002
875 <https://doi.org/10.1111/j.1471-8286.2006.01428.x>

- 876 **Laurenzano C, Mantelatto FLM, Schubart CD.** 2013. South American homogeneity versus
877 Caribbean heterogeneity: populations genetic structure of the western Atlantic fiddler crab
878 *Uca rapax* (Brachyura, Ocypodidae). *Journal of Experimental Marine Biology and*
879 *Ecology* 449:22–27 <https://doi.org/10.1016/j.jembe.2013.08.007>
- 880 **Lefébure T, Douady CJ, Gouy M, Gibert J.** 2006. Relationship between morphological and
881 molecular divergence within Crustacea: Proposal of a molecular threshold to help species
882 delimitation. *Molecular Phylogenetics and Evolution* 40(2006):435–447
883 <https://doi.org/10.1016/j.ympev.2006.03.014>
- 884 **Leigh WJ, Bryant D.** 2015. POPART: full-feature software for haplotype network construction.
885 *Methods in Ecology and Evolution* 6:1110–1116 <https://doi.org/10.1111/2041-210X.12410>
- 886 **Manning RB.** 1993. Three genera remove from the synonymy of *Pinnotheres* Bosc, 1802
887 (Brachyura: Pinnotheridae). *Proceedings of the Biological Society of Washington* 106(3):
888 523–531.
- 889 **Mantelatto FL, Carvalho FL, Simões SM, Negri M, Souza-Carvalho EA, Terossi M.** 2016.
890 New primers for amplification of cytochrome c oxidase subunit I barcode region designed
891 for species of Decapoda (Crustacea). *Nauplius* 24:e2016030 [https://doi.org/10.1590/2358-](https://doi.org/10.1590/2358-2936e2016030)
892 [2936e2016030](https://doi.org/10.1590/2358-2936e2016030)
- 893 **Matzen da Silva J, Creer S, dos Santos A, Costa AC, Cunha MR, Costa FO, Carvalho GR.**
894 2011. Systematic and evolutionary insights derived from mtDNA COI barcode Diversity in
895 the Decapoda (Crustacea: Malacostraca). *PloS ONE* 6(5):1–15, e19449
896 <https://doi.org/10.1371/journal.pone.0019449>

- 897 **Melo GAS, BoehsG.** 2004. Rediscovery of *Holothuriophilus tomentosus* (Ortmann) comb. nov.
898 (Crustacea, Brachyura, Pinnotheridae) in the Brazilian coast. *Revista Brasileira de*
899 *Zoologia* 21(2): 229–232 <https://doi.org/10.1590/S0101-81752004000200010>
- 900 **Munguia-Vega A, Jackson A, Marinone SG, Erisman B, Moreno-Baez M, Girón-Nava A,**
901 **Pfister T, Aburto-Oropeza O, Torre J.** 2014. Asymmetric connectivity of spawning
902 aggregations of a commercially important marine fish using a multidisciplinary approach.
903 *PeerJ* 2:e511 <https://doi.org/10.7717/peerj.511>
- 904 **Nauck E.** 1880. Das Kaugerüst der Brachyuren. *Zeitschrift für wissenschaftliche Zoologie*
905 (*Leipzig*) 34:1–69.
- 906 **Nei M, Kumar S.** 2000. *Molecular Evolution and Phylogenetics*. Oxford University Press, New
907 York
- 908 **Ng PKL, Manning RB.** 2003. On two new genera of pea crabs parasitic in holothurians
909 (Crustacea: Decapoda: Brachyura: Pinnotheridae) from the Indo-West Pacific, with notes
910 on allied genera. *Proceedings of the Biological Society of Washington* 116:901–919.
- 911 **Ng PKL, Guinot D, Davie PJF.** 2008. Systema brachyurorum: Part I. An annotated checklist of
912 extant brachyuran crabs of the world. *The Raffles Bulletin of Zoology* 17:1–286.
- 913 **Nobili G.** 1901. Decapodi raccolti dal Dr. Filippo Silvestri nell' America meridionale. *Bollettino*
914 *del Musei di Zoologia ed Anatomia comparata della R. Univerith di Torino* 16(402):1–16.
- 915 **Ocampo EH, Nuñez JD, Cledón M, Baeza JA.** 2012. Host-specific reproductive benefits, host
916 selection behaviour and host use pattern of the pinnotherid crab *Calyptraeotheres granthi*.
917 *Journal of Experimental Marine Biology and Ecology* 429: 36–46
918 <https://doi.org/10.1016/j.jembe.2012.06.009>

- 919 **Ocampo EH, Nuñez JD, Lizarralde MS, Cledón M.** 2011. Larval development of
920 *Calyptraeotheres garthi* (Fenucci, 1975) (Brachyura, Pinnotheridae) described from
921 laboratory-reared material, with notes of larval character use on Pinnotheridae systematics.
922 *Helgoland Marine Research* 65:347–359 <https://doi.org/10.1007/s10152-010-0228-x>
- 923 **Ocampo EH, Robles R, Terossi M, Nuñez JD, Cledón M, Mantelato FL.** 2013. Phylogeny,
924 phylogeography, and systematics of the American pea crab genus *Calyptraeotheres*,
925 Campos, 1990, inferred from molecular markers. *Zoological Journal of the Linnean*
926 *Society* 169:27–42 <https://doi.org/10.1111/zoj.12045>
- 927 **Ortmann AE.** 1894. Die Decapoden-Krebse des Strassburger Museums, mit besonderer
928 Berücksichtigung der von Herrn Dr. Döderlein bei Japan und bei den Liu-Kiu-Inseln
929 gesammelten und zur zeit im Strassburger Museum aufbewahrten Formen. Theil VII.
930 Abteilung Brachyura (*Brachyura genuina* Boas), II. Unterabteilung: Cancroidea, 2.
931 Section: Cancrinea, 1. Gruppe: Cyclometopa. In: Spengel, S.W. (Ed.) *Zoologische*
932 *Jahrbücher, Abtheilung für Systematik, Geographie und Biologie der Thiere*. Verlag Von
933 Gustav Fischer, Jena. Pp. 411–495, pl. 17 <https://doi.org/10.5962/bhl.part.24064>
- 934 **Palacios-Theil E, Cuesta JA, Felder DL.** 2016. Molecular evidence for non-monophyly of the
935 pinnotheroid crabs (Crustacea: Brachyura: Pinnotheroidea), warranting taxonomic
936 reappraisal. *Invertebrate Systematics* 30:1–27 <https://doi.org/10.1071/IS15023>
- 937 **Paz-Garcia DA, Chávez-Romo HE, Correa-Sandoval F, Reyes-Bonilla H, López-Pérez A,**
938 **Medina-Rosas P, Hernández-Cortés MP.** 2012. Genetic connectivity patterns of corals
939 *Pocillopora damicornis* and *Porites panamensis* (Anthozoa: Scleractinia) along the West
940 Coast of Mexico. *Pacific Science* 66(1): 43–61 <https://doi.org/10.2984/66.1.3>

- 941 **Perez-Miguel M, Drake P, García Raso EJ, Mamán-Menéndez J, Navas IJ, Cuesta AJ.**
942 2019. European Pinnotheridae (Crustacea, Decapoda, Brachyura): species, distribution,
943 host use and DNA barcode. *Marine Biodiversity* 49:57–68 [https://doi.org/10.1007/s12526-](https://doi.org/10.1007/s12526-017-0754-8)
944 [017-0754-8](https://doi.org/10.1007/s12526-017-0754-8)
- 945 **Poeppig E.** 1836. Crustacea Chilensia nova aut minus nota descripsit. *Archiv Für*
946 *Naturgeschichte* 2(1):133–145.
- 947 **Posada D, Buckley TR.** 2004. Model selection and model averaging in phylogenetics:
948 advantages of Akaike information criterion and Bayesian approaches over Likelihood
949 Ratio Test. *Systematic Biology* 53(5):739–808
950 <https://doi.org/10.1080/10635150490522304>
- 951 **Prieto-Rios, E, Solís-Marín FA, Borrero-Pérez GH, Díaz-Jaimes P.** 2014. Filogeografía de
952 Holothuria (*Halodeima*) *inornata* Semper, 1868 (Echinodermata: Holothuroidea). *Revista*
953 *Peruana de Biología* 21(2):155–162 <https://doi.org/10.15381/rpb.v21i2.9818>
- 954 **Prosser S, Martínez-Arce A, Elías-Gutiérrez M.** 2013. A new set of primers for COI
955 amplification from freshwater microcrustaceans. *Molecular Ecology Resources* 13:1151–
956 1155 <https://doi.org/10.1111/1755-0998.12132>
- 957 **Rambaut A.** 2016. FigTree Tree figure drawing tool version 1.4.3. Institute of Evolutionary
958 Biology, University of Edinburgh. Available from: <http://tree.bio.ed.ac.uk/> (accessed 5
959 January 2019).
- 960 **Ramírez-Soriano A, Ramos-Onsins SE, Rozas J, Calafell, F, Navarro A.** 2008. Statistical
961 power analysis of neutrality test under demographic expansions, contractions and
962 bottlenecks with recombination. *Genetics* 179:555–567
963 <https://doi.org/10.1534/genetics.107.083006>

- 964 **Ramos-Onsins SE, Rozas J.** 2002. Statistical properties of new neutrality test against
965 population growth. *Molecular Biology and Evolution* 19:2092–2100
966 <https://doi.org/10.1093/oxfordjournals.molbev.a004034>
- 967 **Rathbun MJ.** 1904. Description of three new species of American crabs. *Proceedings of the*
968 *Biological Society of Washington* 4(17):161–162.
- 969 **Rathbun MJ.** 1918. The grapsoid crabs of America. *Bulletin of the United States National*
970 *Museum* 97:1–461 <https://doi.org/10.5479/si.03629236.97.i>
- 971 **Ratnasingham S, Hebert PDN.** 2013. A DNA-based registry for all animal species: The
972 Barcode Index Number (BIN) system. *PLoS ONE* 8(7):e66213
973 <https://doi.org/10.1371/journal.pone.0066213>
- 974 **Rossi N, Mantelatto FL.** 2013. Molecular analysis of the freshwater prawn *Macrobrachium*
975 *olfersii* (Decapoda, Palaemonidae) supports the existence of a single species throughout its
976 distribution. *PLoS ONE* 8(1):e54698 <https://doi.org/10.1371/journal.pone.0054698>
- 977 **Rozas J, Ferrer-Mata A, Sánchez-DelBarrio JC, Guirao-Rico S, Librado P, Ramos-Onsins**
978 **SE, Sánchez-García A.** 2017. DnaSP v6: DNA Sequence Polymorphism Analysis of
979 Large Datasets. *Molecular Biology and Evolution* 34:3299–3302
980 <https://doi.org/10.1093/molbev/msx248>
- 981 **Rozas J, Sánchez-Delbarrio JC, Messeguer X, Rozas R.** 2003 DnaSP, DNA polymorphism
982 analyses by the coalescent and other methods. *Bioinformatics* 19:2496–2497
983 <https://doi.org/10.1093/bioinformatics/btg359>
- 984 **Salgado-Barragán J.** 2015. A new species of *Pinnixa* (Crustacea: Brachyura: Pinnotheridae)
985 from Mazatlan, Sinaloa, Mexico. *Revista Mexicana de Biodiversidad* 86(3):629–636
986 <http://dx.doi.org/10.1016/j.rmb.2015.03.001>

- 987 **Santos-Beltrán C, Salazar-Silva P.** 2011. Holothuroideos (Echinodermata: holoturoidea) de
988 playas rocosas, zona norte de Bahía Banderas, Nayarit, México. *Ciencia y Mar* 15(45):3–
989 11.
- 990 **Sakai T.** 1939. Studies on the crabs of Japan. IV. Brachygnatha. Brachyrhyncha. Yokendo Co.,
991 Ltd. pp. 365–741. pls. 42–111.
- 992 **Schmitt WL, McCain JC, Davidson ES.** 1973. Fam. Pinnotheridae, Brachyura I: Decapoda I.
993 In: Gruner HE, Holthuis LB, eds. *Crustaceorum Catalogus* 3:1–160.
- 994 **Solís-Marín FA, Arriaga-Ochoa JA, Laguarda-Figueras A, Frontana-Uribe SC, Durán-**
995 **González A.** 2009. *Holoturoideos (Echinodermata: Holothuroidea) del Golfo de*
996 *California*. CONABIO-UNAM-ICMyL, México, 177 pp.
- 997 **Spielmann G, Diedrich J, Haszprunar G, Busch U, Huber I.** 2019. Comparison of three DNA
998 marker regions for identification of food relevant crustaceans of the order Decapoda.
999 *European Food Research and Technology*, 245:987-995 [https://doi.org/10.1007/s00217-](https://doi.org/10.1007/s00217-018-3199-9)
1000 [018-3199-9](https://doi.org/10.1007/s00217-018-3199-9)
- 1001 **Takeda M, Masahito P.** 2000. Systematic notes on the pinnotherid crabs of the genus
1002 *Pinnaxodes* (Crustacea: Decapoda: Brachyura). *Bulletin of Natural Science Museum of*
1003 *Tokyo Serie A* 26(3):99–112.
- 1004 **Tamura K, Stecher G, Peterson D, Filipski A, Kumar S.** 2013. MEGA6: Molecular
1005 Evolutionary Genetics Analysis version 6.0. *Molecular Biology and Evolution* 30:2725–
1006 2729 <https://doi.org/10.1093/molbev/mst197>
- 1007 **Tesch JJ.** 1918. The decapoda brachyura of the Siboga expedition Goneplacidae and
1008 Pinnotheridae. *Siboga Expéditie* 39:149–296 <https://doi.org/10.5962/bhl.title.10267>

- 1009 **Wares JP, Gaines SD, Cunningham, CW.** 2001. A comparative study of asymmetric migration
1010 events across a marine biogeographic boundary. *Evolution* 55:295–306
1011 <https://doi.org/10.1111/j.0014-3820.2001.tb01294.x>
- 1012 **Will WK, Rubinoff D.** 2004. Myth of the molecule: DNA barcodes for species cannot replace
1013 morphology for identification and classification. *Cladistics* 20:47–55
1014 <https://doi.org/10.1111/j.1096-0031.2003.00008.x>
- 1015 **Zhang C, Li Q, Wu X, Liu Q, Cheng Y.** 2017. Genetic diversity and genetic structure of
1016 farmed and wild Chinese mitten crab (*Eriocheir sinensis*) populations from three major
1017 basins by mitochondrial DNA COI and Cyt b gene sequences. *Mitochondrial DNA PART A*
1018 2–9 <https://doi.org/10.1080/24701394.2017.1404048>
- 1019 **Zhou H, Xu J, Yang M, Wu B, Yan B, Xiong Y.** 2015. Population genetic diversity of
1020 sesarmid crab (*Perisesarma bidens*) in China based on mitochondrial DNA. *Mitochondrial*
1021 *DNA, Early Online* 1–8 <https://doi.org/10.3109/19401736.2015.1015002>
- 1022

Figure 1

Holothuriophilus trapeziformis Nauck, 1880

A-C, male from playa Panteón, Oaxaca, Mexico (UMAR-DECA-308): A, dorsal view; B, ventral view; C, frontal view. D-F, female from playa Agua Blanca, Oaxaca, Mexico (UMAR-DECA-307): D, dorsal view; E, ventral view; F, frontal view. G, male inside the gut of *Holothuria (Halodeima) inornata*, from playa Pinitos, Sinaloa, Mexico.

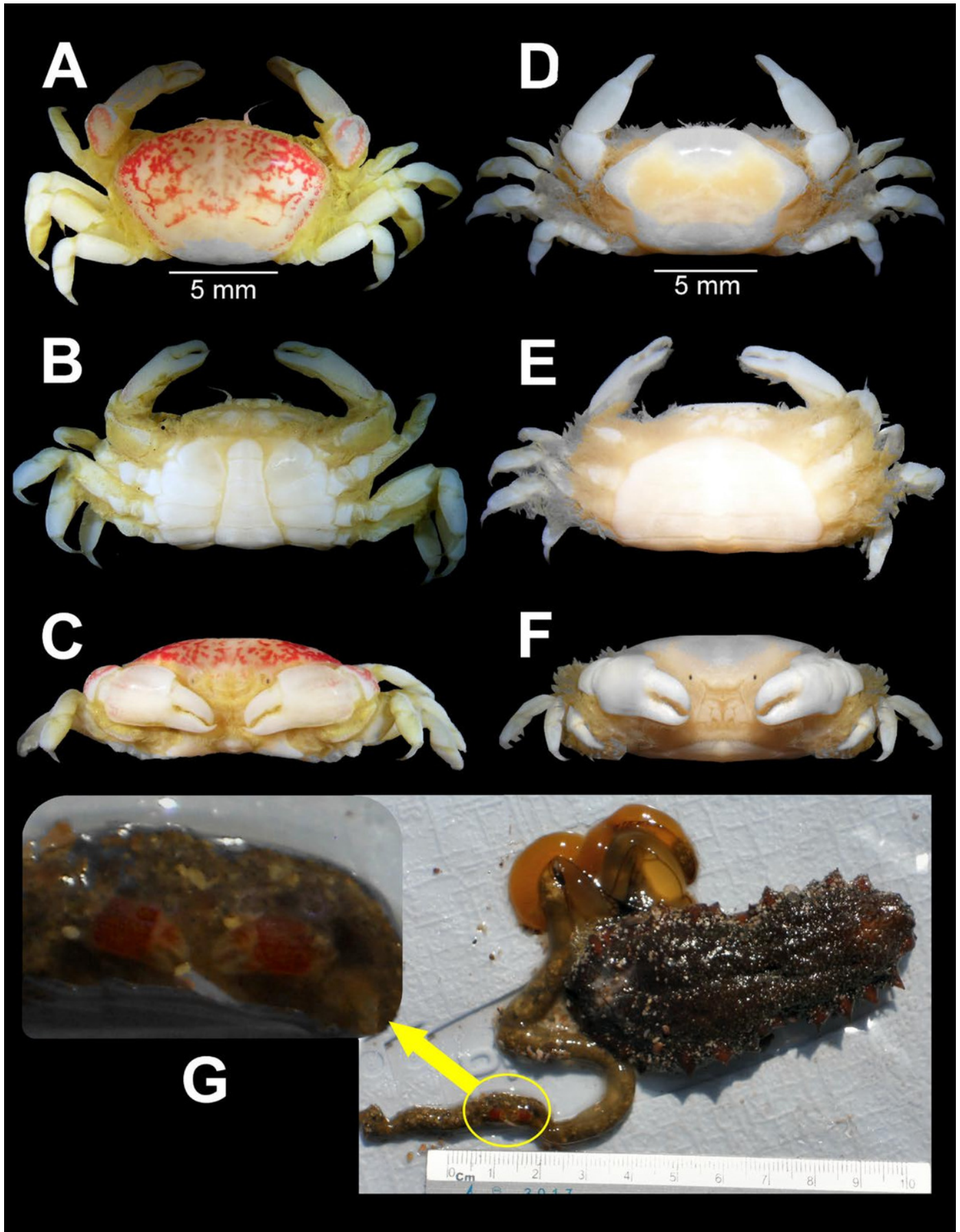


Figure 2

Holothuriophilus trapeziformis Nauck, 1880

A-D, male from playa Panteón, Oaxaca, Mexico (UMAR-DECA-308): A, dorsal view; B, frontal view; C, third-fourth sternal plate; D, abdomen; E, abdominal view of the left first gonopod; F, abdominal view of the left second gonopod; A, C, hollow circles indicating pits. Fine dots indicating pilosity. A-D, half of the illustration without ornamentation.

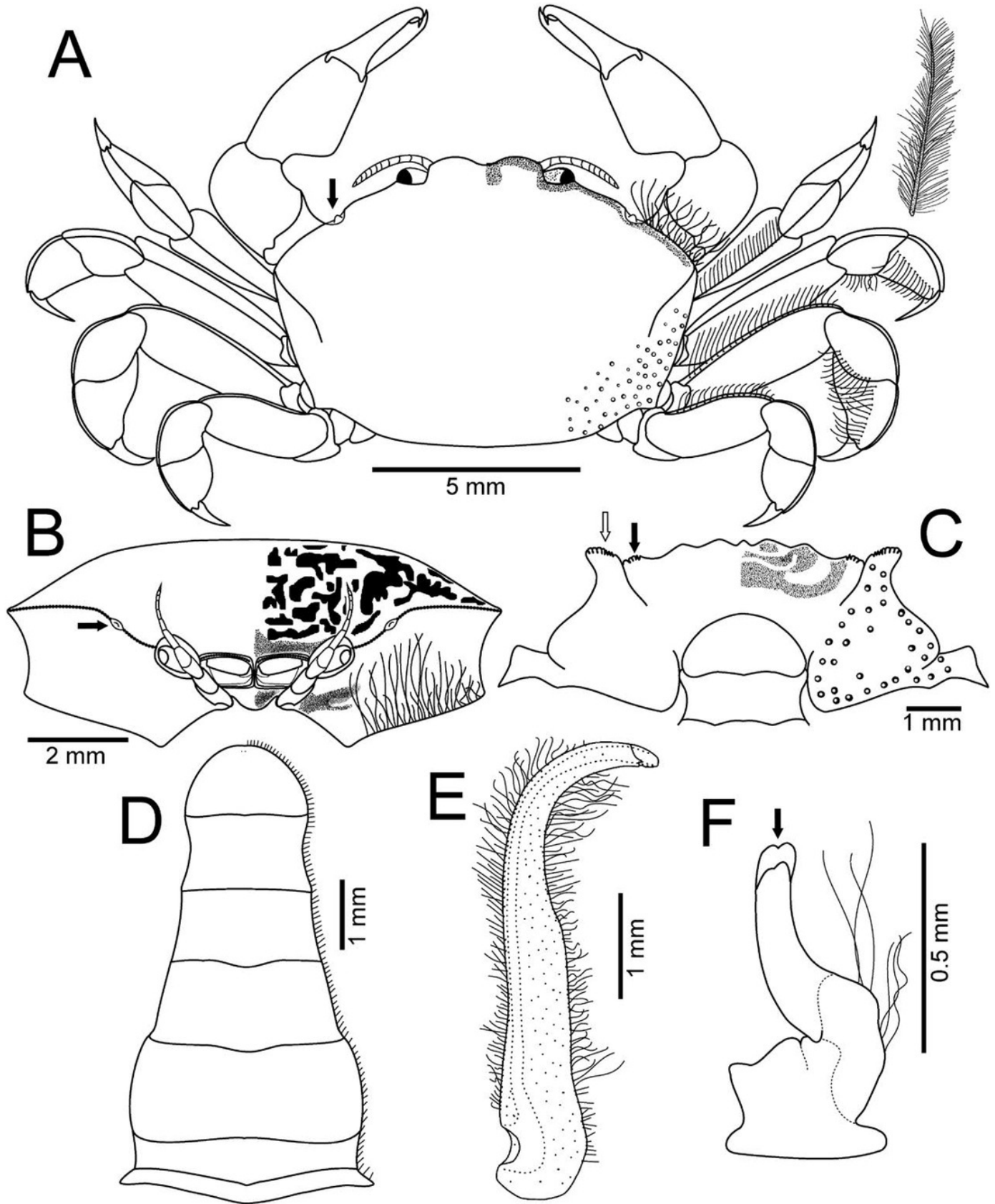


Figure 3

Holothuriophilus trapeziformis Nauck, 1880

A, antenna. B, antennule: a, superior palp; b, inferior palp; C, second maxilliped: a, endopod; b, exopod; c, exopod flagellum; D, third maxilliped: a, ischiomerus; b, carpus; c, propodus; d, dactylus; bold arrow indicating a projection. E, exopod of the third maxilliped. F, chela; bold arrow indicating mid-posterior teeth; dotted arrow, indicating the lamella; dashed arrow, indicating granules.

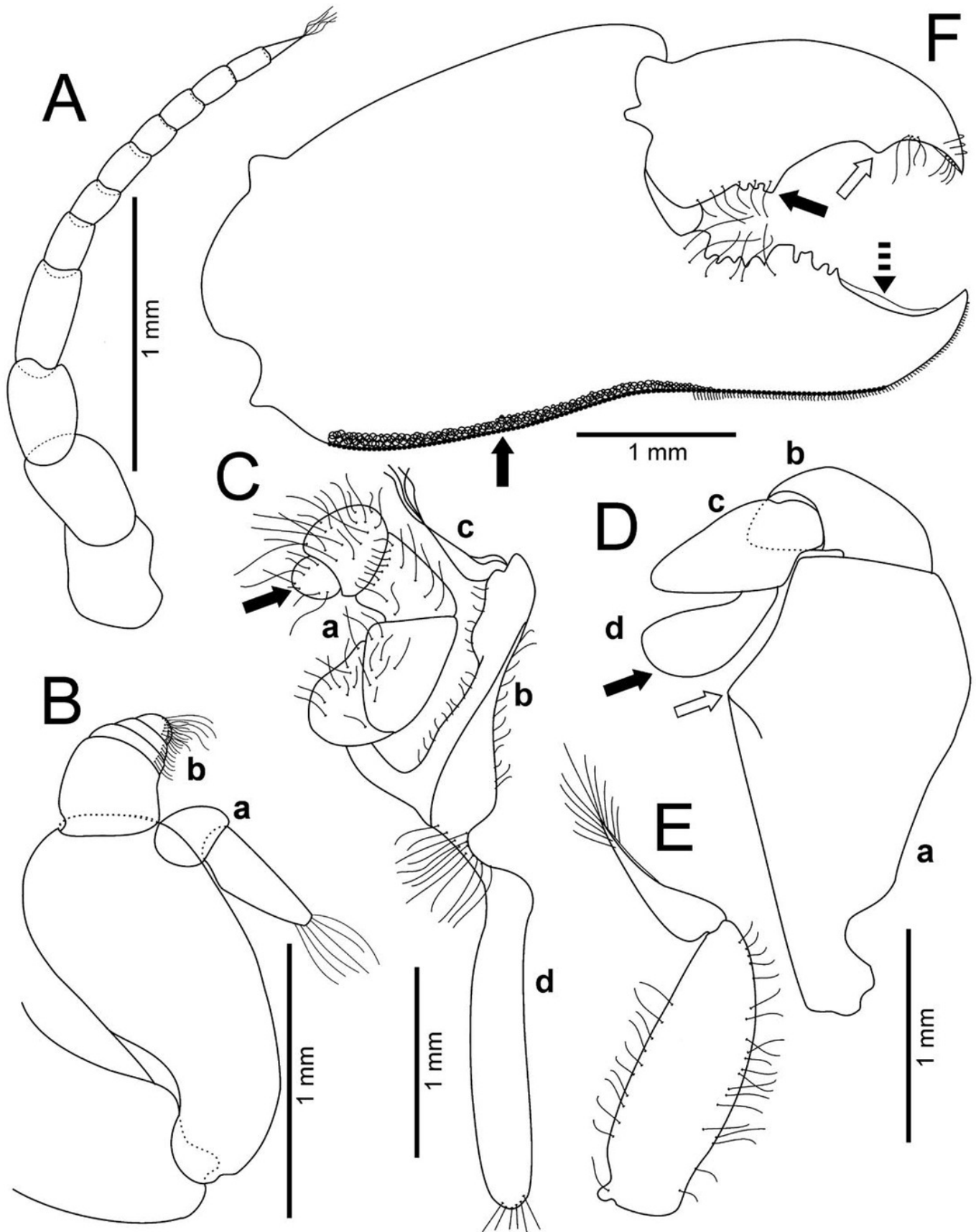


Figure 4

Comparison between males of *Holothuriophilus trapeziformis* Nauck, 1880 from the Pacific coast of Mexico

A-D, Sinaloa (DECA-1190; CW= 8 mm); E-H, Guerrero (DECA-1148; CW= 8 mm); I-L, Oaxaca (DECA-1270; CW= 8 mm). A, E, I, carapace outline; B, F, J, right chela, external view; C, G, K, left Mxp3 endopod, external view; D, H, L, first gonopod, abdominal view; e, gonopod tip, abdominal view; f, gonopod tip, sternal view.

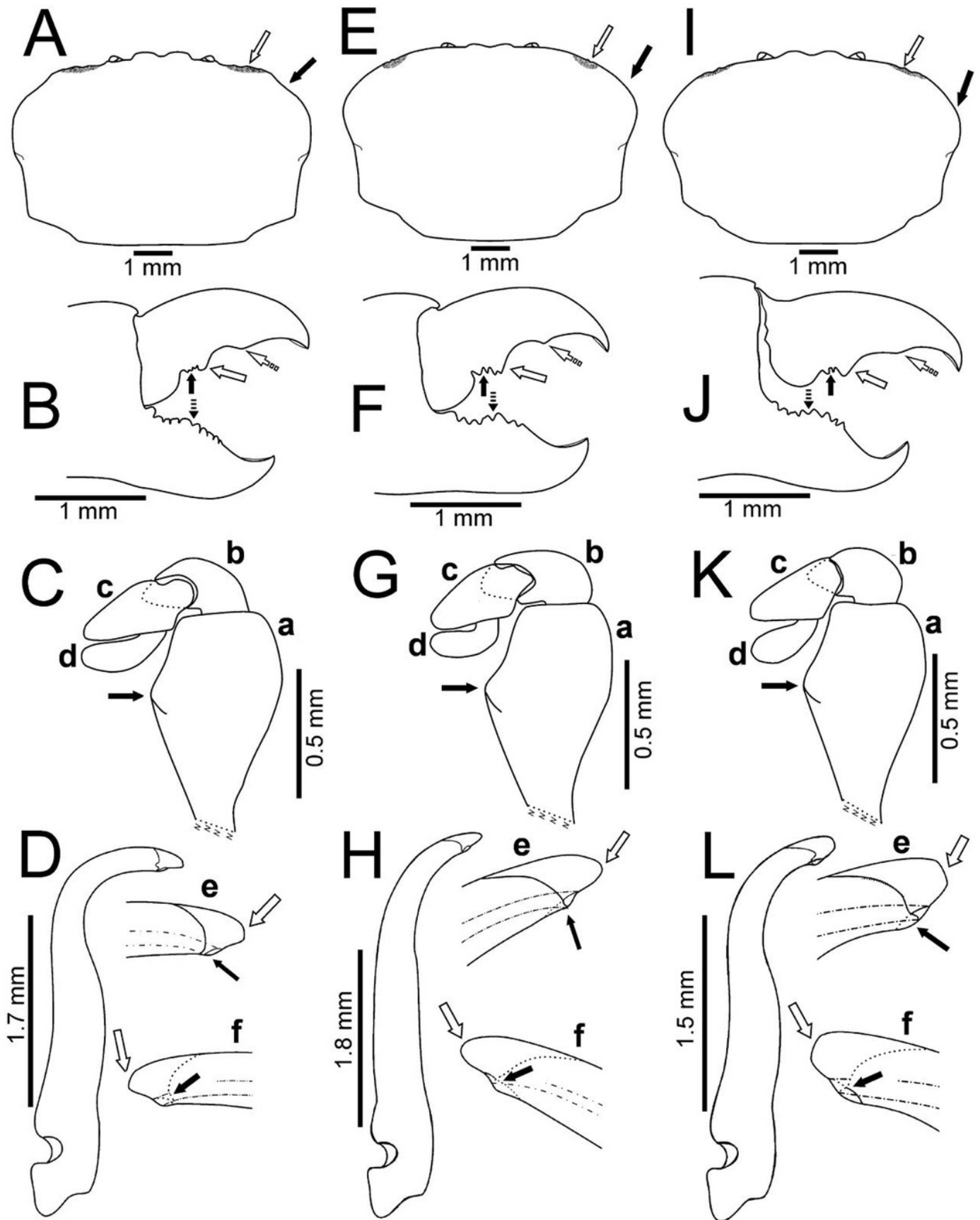


Figure 5

Comparison between ovigerous females of *Holothuriophilus trapeziformis* Nauck, 1880 from the Pacific coast of Mexico

A-C, Sinaloa (UMAR-DECA-1192; CW= 8 mm); D-F, Guerrero (DECA-1149; CW= 8 mm); G-I, Oaxaca (UMAR-DECA-1182; CW= 8 mm); J, K, chelae, external view, Oaxaca (UMAR-DECA-1172; CW= 9 mm). A, D, G, carapace outline; B, E, H, right chela, external view; C, F, I, left Mxp3 endopod, external view.

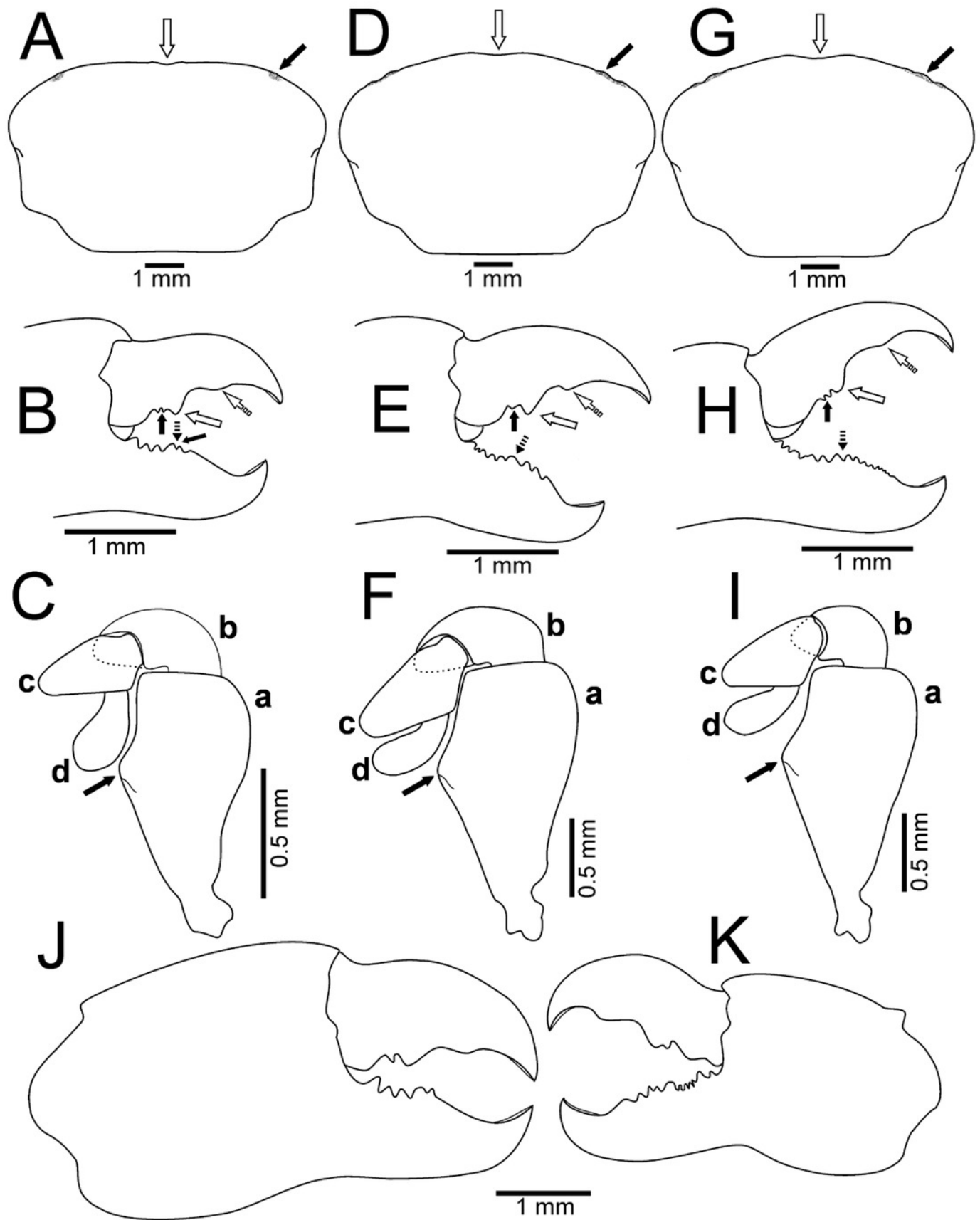


Figure 6

Comparison between females of *Holothuriophilus trapeziformis* Nauck, 1880 and *H. pacificus* (Poepig, 1836)

A, carapace; B, third maxilliped; C, chela; D, ovigerous abdomen. E-H, *H. pacificus* holotype of from San Vicente, Chile (Taken from Garth 1957): E, carapace; F, third maxilliped; G, chela; H, abdomen. I-J, lectotype of *H. trapeziformis* from Mazatlán, Mexico (Taken from Ah Yong & Ng 2007): I, dorsal view of carapace; J, third maxilliped. K, *H. trapeziformis* from Guerrero, third maxilliped of the adult female of (Taken from Campos *et al.* 2012). Scale of E= x3.5, F= x18.6, G= x4.6, H= x2.9 (*fide* Garth 1957).

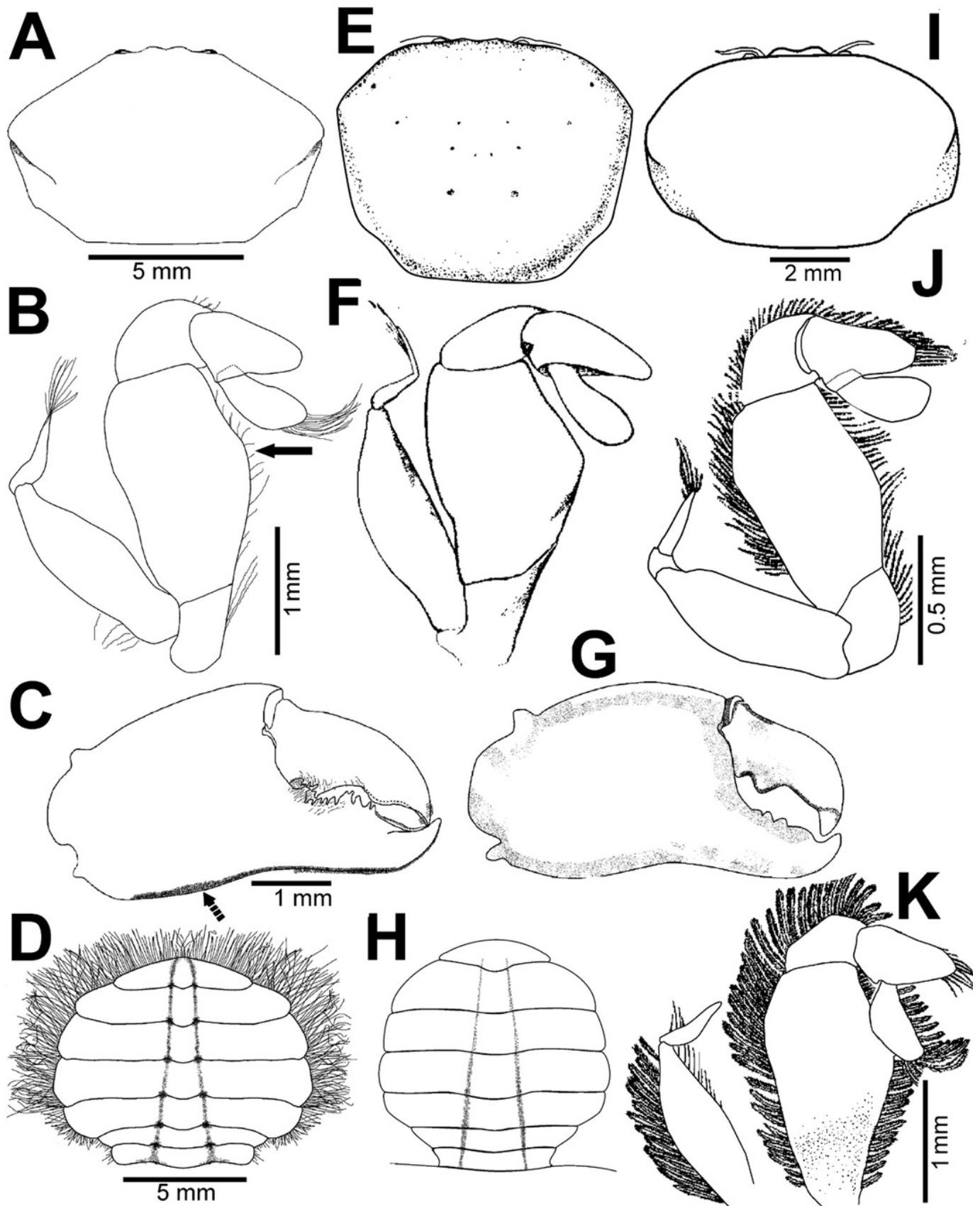


Figure 7

Comparison between males of *Holothuriophilus trapeziformis* Nauck, 1880 and *H. pacificus* (Poepig, 1836)

A, D, third maxilliped; a, dactylus; b, propodus; c, exopod flagellum. B, F, abdomen. C, F, first gonopod. A-C, from playa Panteón, Oaxaca, Mexico; C, abdominal view of the gonopod, Mexico (UMAR-DECA-308). D-F, from Talcahuano, Chile (Taken from Garth 1957).

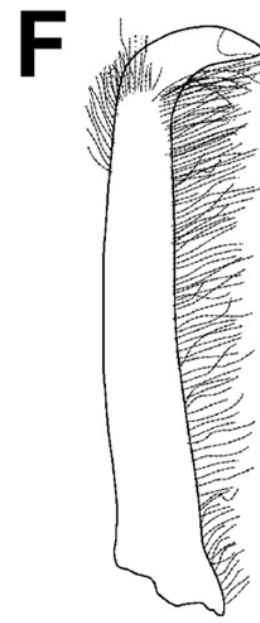
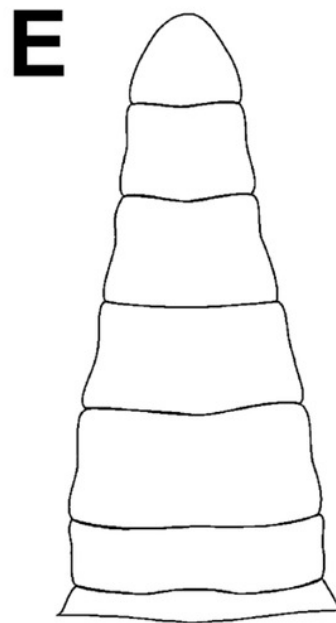
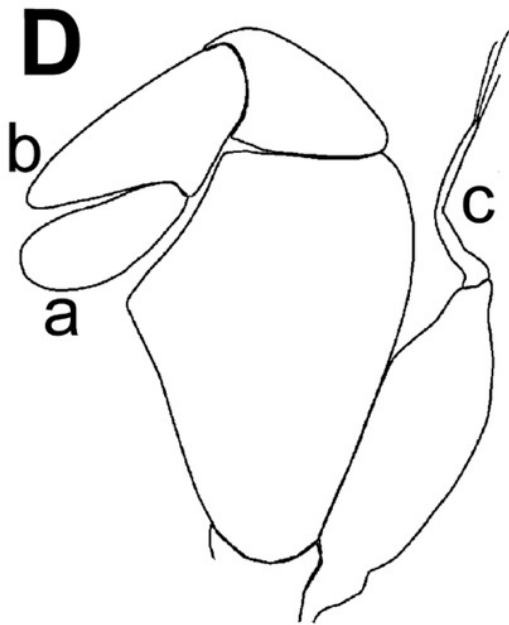
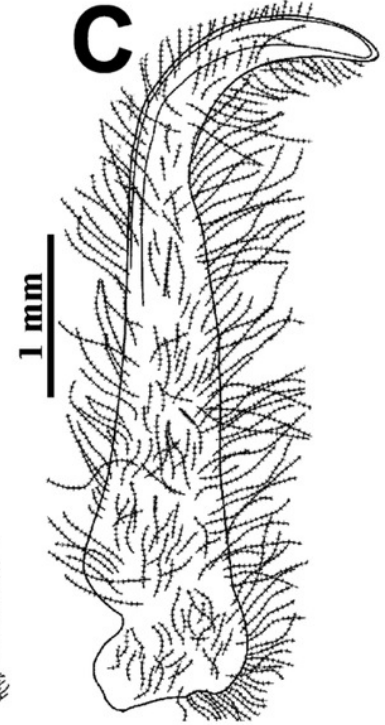
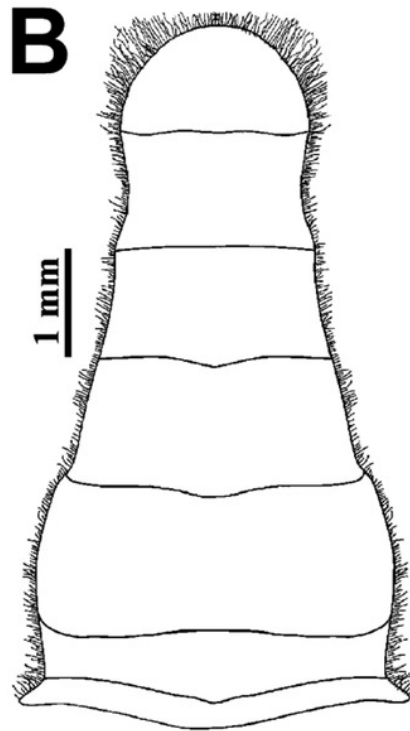
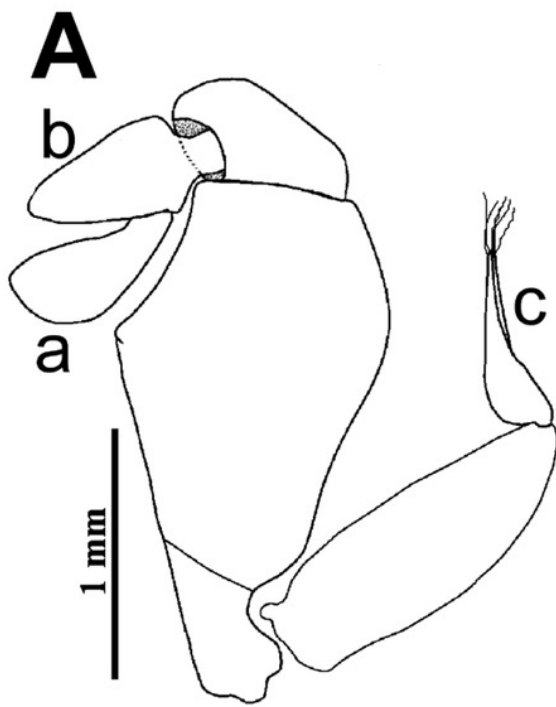


Figure 8

Condensed unrooted Maximum likelihood tree based on mitochondrial cytochrome c oxidase (COI) with the General Time Reversible with gamma distribution (GTR+G) mode

Data: BOLD process ID, species name, associated BIN. Branch values represent bootstrap probabilities (1000 permutations).

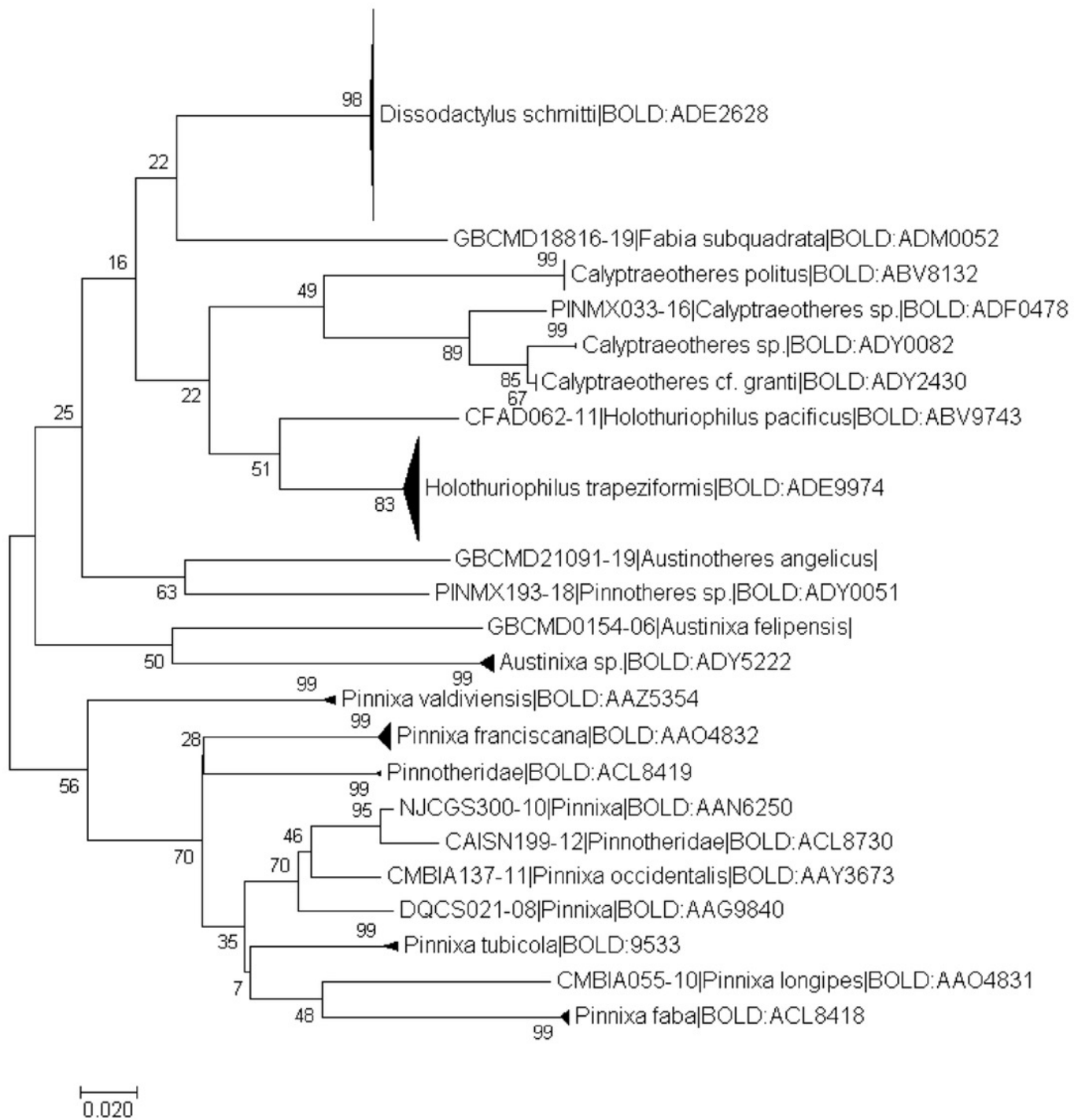


Figure 9

Parsimony haplotype network for 37 COI sequences of *Holothuriophilus trapeziformis* from the Pacific coast of Mexico

Haplotype crossbars represent nucleotide substitutions between haplotypes based on a 567 bp sequences. Each circle indicates a unique haplotype and variation in size circle reflects the number of sequences assigned to it. Size of circles represent the number of individuals and colors the region to which it belongs. Dotted circle represents a missing haplotype.

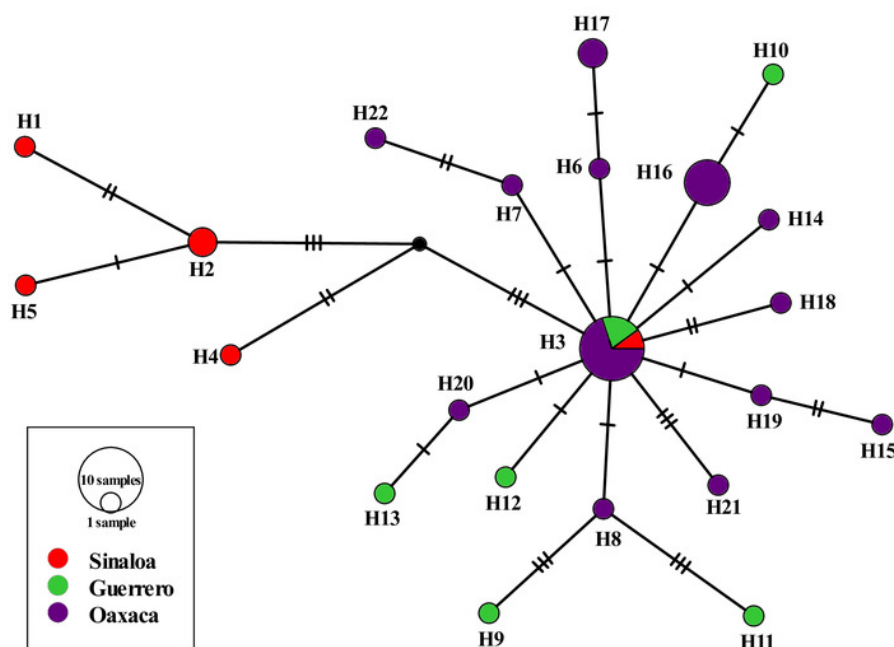


Figure 10

Figure 10. Mismatch distribution of *Holothuriophilus trapeziformis*

A, overall Mexico population sample; B, Sinaloa; C, Guerrero; D, Oaxaca.

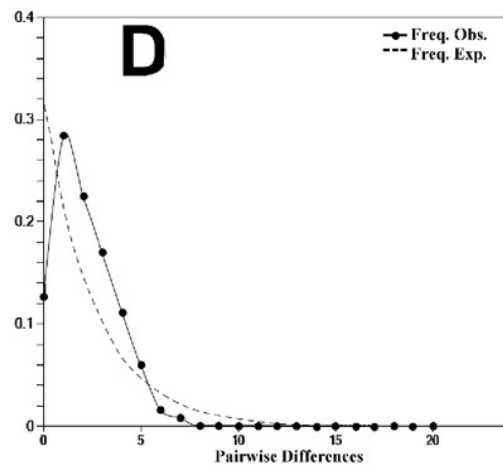
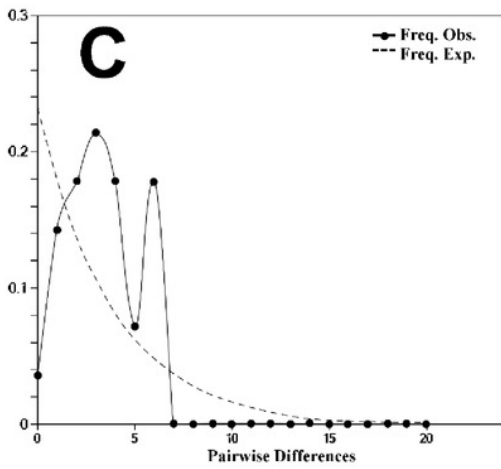
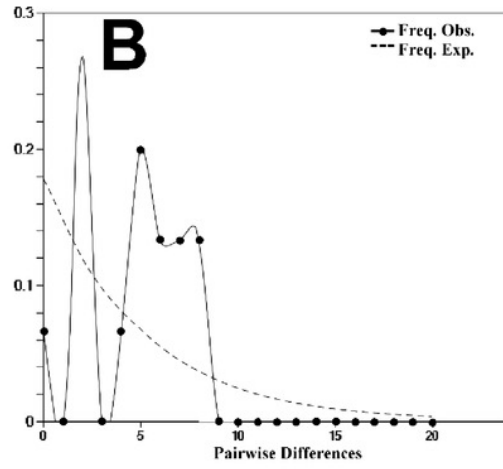
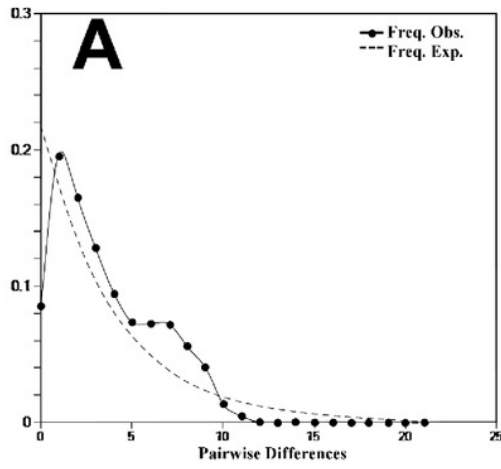


Table 1 (on next page)

Gen diversity estimations based on 501 bp of the COI sequences of *Holothuriophilus trapeziformis* examined in this study

Number of sequences (n), number of segregating sites (S), number of transitions and transversions (T/t), mean number of nucleotide differences between pairs of sequences (k), number of haplotypes (h), haplotype diversity (Hd), nucleotide diversity (π), guanine-cytosine content (G+C), neutrality test (Tajima's D and Fu's Fs) and demographic tests (r, and R2). * = $p < 0.05$.

1

Region	n	S	T/ t	k	h	Hd±SD	π ±SD	G+ C	D	Fs	r	R2
Mexico	37	33	28/6	3.775± 1.946	22	0.914± 0.036	0.00716± 0.0011	0.348	- 1.834 64*	- 13.45 301*	0.07780	0.11407*
Sinaloa	61	12	9/2	4.267± 2.45	55	0.933± 0.122	0.00902± 0.0021	0.351	- 0.691 53	- 0.629 89	0.22104	0.20112*
Guerero	82	12	10/2	3.286± 1.887	77	0.964± 0.077	0.00656± 0.0014	0.347	- 1.459 38	- 2.988 45*	0.15286	0.18034*
Oaxaca	23	17	13/3	2.047± 1.191	12	0.874± 0.052	0.00393± 0.0007	0.345	- 1.897 23*	- 6.707 87*	0.08442	0.12867*

2

Table 2 (on next page)

Haplotypes and haplotype frequencies based on COI sequences for *Holothuriophilus trapeziformis* from the Pacific coast of Mexico

Sin, Sinaloa; Gro, Guerrero, Oax, Oaxaca.

Haplotype (H)	Sequence	Haplotype frequency		
		Sin	Gro	Oax
H 1	TAATTCGCTTGGAAATACAACGCTTTCCCAGCT	1	0	0
H 2	TAACCCGCTTGGAAATACAACGCTTTCCCAGCT	2	0	0
H 3	TAACCTACATGGAAATACAGCACTTACCCAGCT	1	2	7
H 4	TAACCTGCATGGAAGTACAACACTTTCCCAACT	1	0	0
H 5	TAACCCGCTTGGAAATACAACGCTTTTCCAGCT	1	0	0
H 6	TGACCTACATGGAAATACAGTGCTTACCCAGTT	0	1	0
H 7	TAACCTACATGGTAATACAGCACTTACCCAGCC	0	1	0
H 8	TAGCCTACATGGAAATACAGCACTTACCCAGCT	0	1	0
H 9	TAACCTACATGGAAATACAGCATTTACCCGGCT	0	1	0
H 10	TAACCTACATGGAAATAAAACACCTACCCAGTT	0	1	0
H 11	TAACCTACATGGAAATACAGCACTTACCCAGTT	0	1	0
H 12	TAACCTACATGGAAATACAGCACTTACCCGGCT	0	0	5
H 13	TAACCTACATGAAAATACAGCACTTACCCAGCT	0	0	1
H 14	TAACCTACATGGTAATACAGCACTTACCCAGCT	0	0	1
H 15	TAACCTACATGGAAATACAGCACTTAACCAGCT	0	0	1
H 16	TAACCTACATGAAAACACAGCACTTACCCAGCT	0	0	2
H 17	TAACCTACATGGAAATACGGCACTCACCCAGCT	0	0	1
H 18	TAACCTACATGGAAATACAGCACTTAATCAACT	0	0	1
H 19	TAACCTACACAGAGATACAGCACTTACCCAGCT	0	0	1
H 20	GAACCTACATGGAAATACAGCACTTACCCAGCT	0	0	1
H21	TAACCTACATGGAAATGCAGCACTTACCCAGCT	0	0	1
H 22	TAACCTATATGGAAATGCAGCACTTACCTAGCT	0	0	1
Total		6	8	23

Table 3(on next page)

Spatial Analyses of the Molecular Variance (SAMOVA) for COI sequences of *Holothuriophilus trapeziformis* from the Pacific coast of Mexico

Where k=2 (Group 1: Sinaloa; Group 2: Guerrero-Oaxaca). Statistical significance $p \leq 0.05$.

Source of variation	df	Square sums	Variance component	% Total variance	Fixation indices	<i>p-value</i>
Between localities	1	17.745	1.58021	53.36	ϕ_{CT} 0.53	≤ 0.001
Between localities within groups	1	2.107	0.06680	2.26	ϕ_{SC} 0.04	0.021
Within localities	34	44.688	1.31436	44.38	Φ_{ST} 0.55	≤ 0.001
Total	36	64.541	2.96137			

1

Table 4(on next page)

Spatial Analyses of the Molecular Variance (SAMOVA) for COI sequences of *Holothuriophilus trapeziformis* from the Pacific coast of Mexico

Where $k=1$ (Group 1: Sinaloa; Group 2: Guerrero-Oaxaca). Statistical significance $p \leq 0.05$.

Source of variation	df	Square sums	Variance component	% Total variance	Fixation indices	<i>p-value</i>
Between localities	2	19.852	0.86117	39.58	Φ_{ST} 0.39	
Within localities	34	44.688	1.31436	60.42		
Total	36	64.541	2.1755			

1